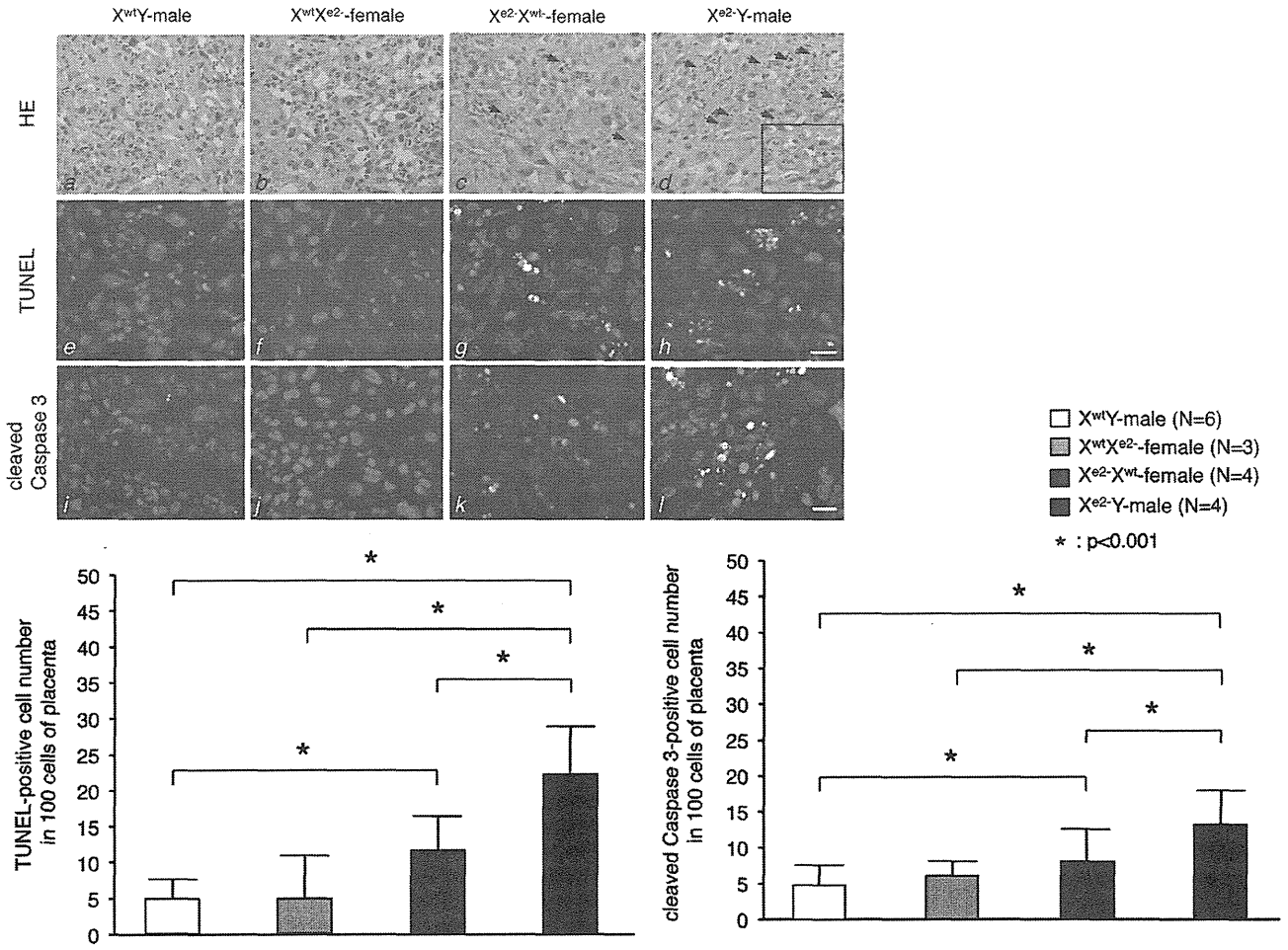


FIGURE 3. ***MeCP2_e2* deficiency results in placenta abnormalities.** The *top panels* (*a–d*) show placenta sections stained with hematoxylin and eosin. The *inset* shows the section at higher magnification. *Arrows* show apoptotic cells. The *middle panels* (*e–h*) show TUNEL staining of the same sections. Apoptotic nuclei appear as multiple spots (*yellow*), indicating DNA fragmentation. Propidium iodide was used as counterstain. The *bottom panels* (*i–l*) show cleaved caspase-3 immunostaining of the placenta. TUNEL-positive cells are indicated by *arrows*. *Scale bar*, 25 μm. An increase in the number of TUNEL-positive cells and cleaved caspase 3-positive cells was observed in the placentas of $X^{e2-}X^{wt}$ and $X^{e2-}Y$ embryos having a maternal *MeCP2_e2* null allele (refer to *bar graphs* in *lower panel* for quantitation) *, $p < 0.001$; *brackets* and *asterisks* indicate significant differences. *Error bars*, S.D.

cate that MeCP2_e2 is not essential for mediating transcriptional silencing of MeCP2 target genes in the brain.

*Parent-specific Effects of MeCP2_e2 Null Allele Birth Rates*—We next examined whether *MeCP2_e2* deficiency mediated any other non-neuronal phenotype. Interestingly, we observed reduced births of progeny that carried *MeCP2_e2* null allele of maternal origin. Specifically, we found a 76% reduction in $X^{e2-}Y$ males and a 44% reduction in $X^{e2-}X^{wt}$ females born to $X^{wt}X^{e2-}$ female and wild-type male pairings (Table 1). Similarly, in $X^{e2-}X^{wt}$ and $X^{e2-}Y$ pairings, $X^{e2-}Y$ and $X^{e2-}X^{e2-}$ births were reduced by 50 and 60%, respectively (Table 2). In contrast, birth rates of $X^{wt}X^{e2-}$ females (having a paternal $X^{e2-}$) did not deviate from the expected values (Tables 2 and 3). We exclude the possibility that these were nonspecific effects resulting from toxicity of the tTA in the targeting vector because no such decreases in births were observed in an unrelated transgenic mouse model carrying the same vector backbone.[6] Taken together, these results point to an association between reduced embryo viability and a maternally transmitted *MeCP2_e2* null allele.

To further delineate the time period at which selection against embryos carrying maternal *MeCP2_e2* null alleles occurred, we examined the genotype distribution at 13.5 dpc and observed similar trends (Tables 4 and 5). Moreover, we did not find any evidence of resorbed embryos at this time point (data not shown). We also performed morphological assessment of the uterus at preimplantation and postimplantation stages and found no abnormalities in preimplantation sites and the implantation process (data not shown). Nevertheless, these findings suggest that the reduced number of embryos carrying a mutant maternal *MeCP2_e2* allele is due neither to a failure in implantation nor to embryo lethality at postimplantation but to reduced viability of the embryo prior to implantation or early embryonic lethality after implantation.

*Maternally Transmitted MeCP2_e2 Null Allele Results in Apoptosis and Altered peg-1 Expression in Placenta*—During early development of the female mammal, one of the two X chromosomes becomes transcriptionally inactive to allow dos-

[6] A. Otsuki and A. Kurimasa, unpublished results.

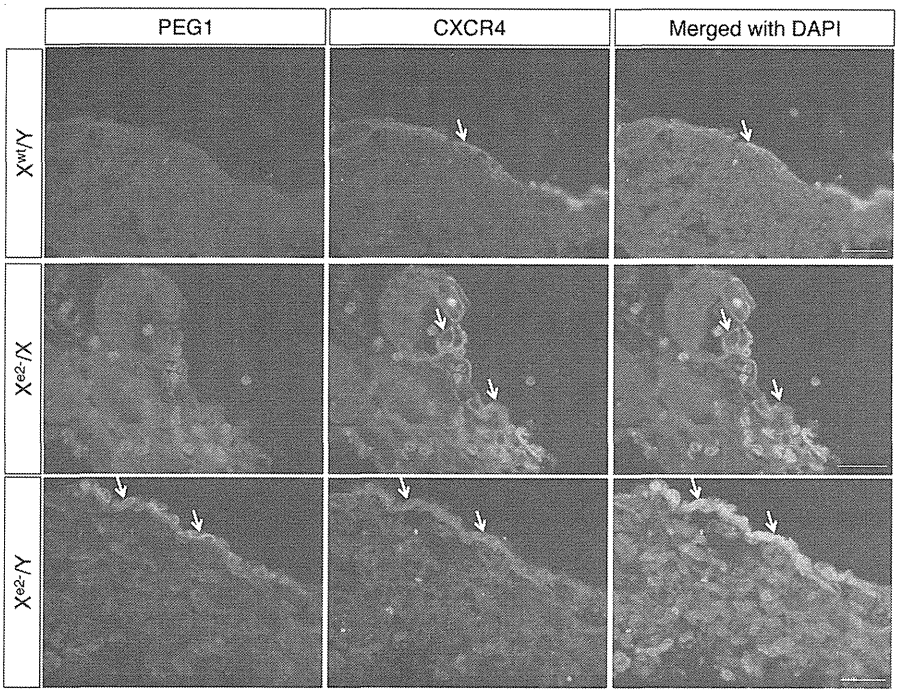


FIGURE 4. **Loss of maternal MeCP2_e2 results in failure to silence *peg-1* expression in trophoblast cells.** CXCR4 is a trophoblast cell marker. $X^{wt}/Y$ and $X^{e2-}X^{wt}$ placenta have minimal *peg-1* expression, whereas $X^{e2-}/Y$ placenta show elevated *peg-1* levels in trophoblast cells (*arrows*). *Scale bars*, 50 $\mu$m.

age compensation of X-linked genes (19, 20). In mouse extraembryonic lineages, such as placenta, the paternally derived X chromosome undergoes preferential inactivation, a phenomenon called imprinted paternal X chromosome inactivation (XCI) (21, 22). Hence, we examined the effect of *MeCP2_e2* deficiency in placenta tissue at 13.5 dpc. Interestingly, placentas of embryos carrying a maternal *MeCP2_e2* null allele exhibited increased apoptosis, which was more notable in placentas of males (Fig. 3). These TUNEL-positive cells expressed peg-1 (supplemental Fig. 1), an imprinted gene known to function in placenta development (23, 24). In contrast, very few apoptotic cells were observed in the placenta of $X^{wt}X^{e2-}$ embryos carrying a paternal *MeCP2_e2* null allele (Fig. 3). In addition, immunostaining revealed increased Peg-1 levels in cells expressing CXCR4, a trophoblast marker (25), in the placenta of animals carrying a maternal *MeCP2_e2* null allele (Fig. 4 and supplemental Fig. 1). Taken together, our results indicate that MeCP2_e2 is essential for the maintenance of *peg-1* silencing in trophoblast cells and that elevated expression of *peg-1* in the placenta has deleterious effects on cell survival.

We also examined transcript levels of *peg-1* and other imprinted genes involved in placenta function, such as *peg-3*, *igf-2*, and *h19* (23). Among these four genes, *peg-1* exhibited elevated transcript levels in the placenta of embryos carrying a maternal mutant allele (Fig. 5*a*), in concordance with our immunohistological findings. The mRNA levels of the other three genes were unchanged (Fig. 5*a*). In placentas of animals carrying the *MeCP2* two-isoform knock-out allele, *peg-1* expression was also elevated (Fig. 5*b*). The *peg-1* transcript levels were not due to deregulation of imprinting in placenta because imprinted paternal XCI was found to be intact in these animals (Fig. 5*c*). Rather, elevated *peg-1* transcript levels directly correlate with the loss of *MeCP2_e2* expression effected by imprinted paternal XCI. These findings indicate that *MeCP2_e2*-specific transcriptional silencing activity is essential for the regulation of *peg-1* expression and possibly of other genes in placenta.

The imprinted gene *peg-1*, located in murine chromosome 6, has been reported to play a role in angiogenesis in extraembryonic tissue (26). Mutations in *peg-1* have also been implicated in placenta failure (24, 25) and embryonic growth retardation (27). One group has reported that paternally expressed transcripts are associated with premature placenta (28). Interestingly, paternal transmission of a *peg-1* null allele in heterozygous mice results in diminished postnatal survival rates, whereas maternal transmission does not generate any remarkable phenotype (27, 29). It is clear from these reports that deregulation of *peg-1* expression or imprinting status has deleterious consequences on embryo viability and placenta function. Our current study demonstrates that MeCP2_e2 is an essential regulator of *peg-1* expression in extraembryonic tissue. As for how increased *peg-1* expression correlates with observed placenta defects in carriers of a maternal *MeCP2_e2* null allele, we propose a scenario wherein perturbations in *peg-1* expression results in disruption of biological pathways that involve Peg-1, leading to enhanced apoptosis in placenta. Peg-1 is a membrane-bound protein that is predicted to have lipase or acyltransferase activity based on sequence homology with the $\alpha/\beta$-hydrolase superfamily of proteins (30). Lipid metabolism is a very important biological process and is critical for the developing embryo and placenta. We propose that loss of *MeCP2_e2* results in failure to transcriptionally silence *peg-1* in extraem-

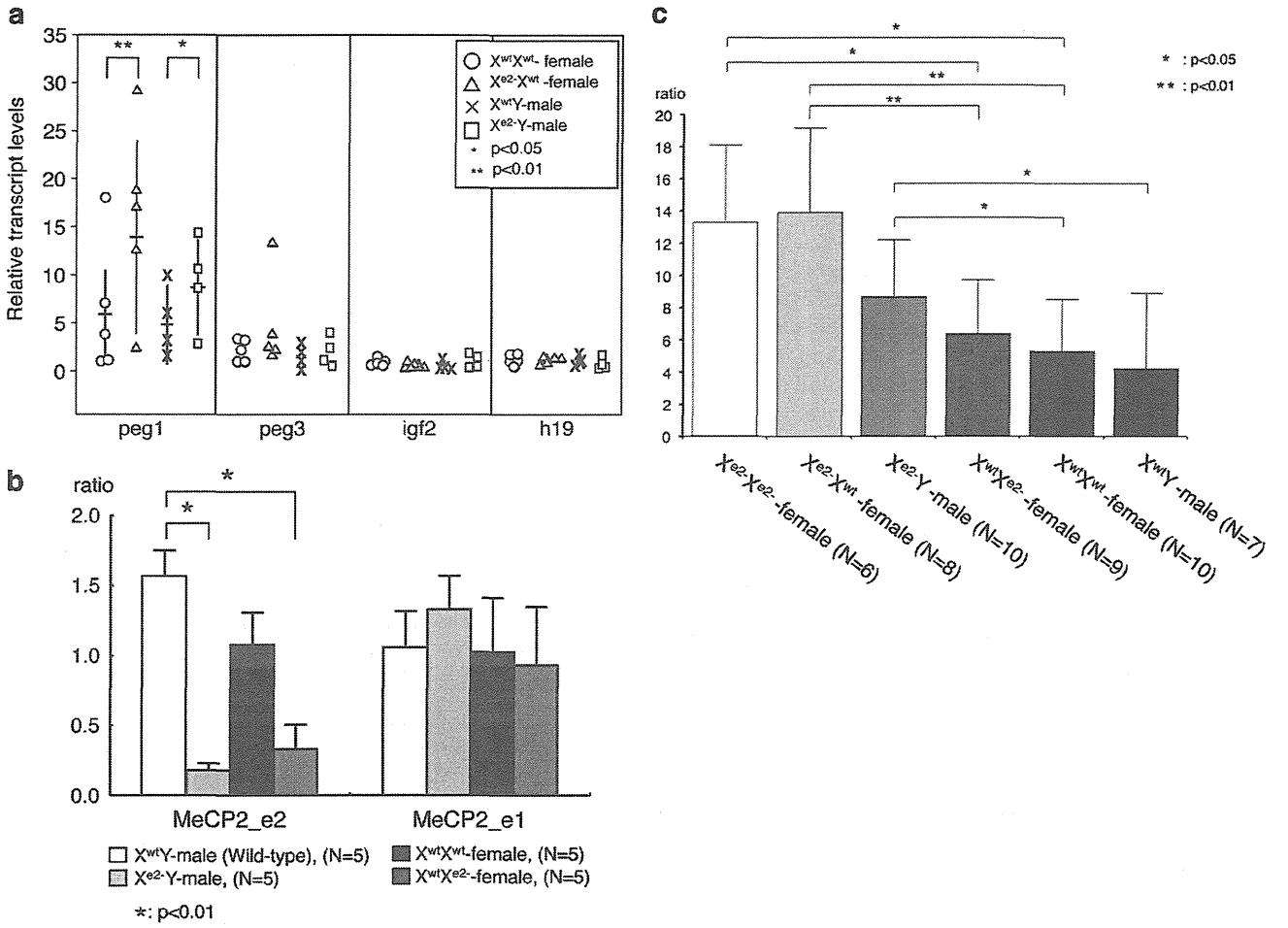


FIGURE 5. **Quantitative PCR analysis of placenta.** Shown are (*a*) placenta transcript levels of selected imprinted genes, *peg-1*, *peg-3*, *igf-2*, and *h19*, from 13.5 dpc embryos and (*b*) placenta transcript levels of peg-1 in *MeCP2_e2* and *MeCP2_e1* (two-isoform knockout) mutants. The *horizontal* and *vertical bars* of *peg-1* transcripts (*a*) show averages and S.D. of each genotype, respectively. *c*, *peg-1* expression in placentas of various genotypes. Maternally derived $X^{e2-}$ allele up-regulated *peg-1* expression. *, $p < 0.05$; **, $p < 0.001$. *Brackets* and *asterisks* indicate significant differences. *Error bars*, S.D.

bryonic tissue, leading to increased Peg-1 enzymatic activity, aberrant regulation of Peg-1 binding partners or downstream targets, and, ultimately, apoptosis.

We have earlier stated that we found the implantation process to be normal for these animals. Moreover, at 13.5 dpc, there was no evidence of resorbed embryos, and the skewed embryo genotypes resembled that from postnatal analysis. These results, taken together with the increased number of apoptotic trophoblast cells and elevated *peg-1* expression in embryos carrying a maternal *MeCP2_e2* null allele, suggest that the loss of *MeCP2_e2* leads to trophoblast dysfunction during preimplantation through abnormal *peg-1* expression. Furthermore, we view the increase in apoptotic trophoblast cells as a persisting phenotype brought about by early perturbation of placenta gene expression. In mice, placental development begins in the blastocyst at embryonic day 3.5 when the trophectoderm layer becomes distinct from the inner cell mass (32). The trophoblast that lines the blastocyst plays an important role during attachment to the endometrium and in the formation of the placenta (31, 32). It has been reported by other groups that trophoblast dysfunction leads to disruption of placenta formation and reduction of birth number (31, 33). In our current study, we have shown that loss of *MeCP2_e2* results in a trophoblast defect that ultimately leads to reduced embryo viability.

Because some carriers of a mutant *MeCP2_e2* allele are born and develop into healthy adults, we hypothesize that the placenta abnormalities in these animals may have been overcome by *de novo MeCP2_e1* compensation or some other adaptation. In some types of extraembryonic cells, XCI can follow either a paternal or maternal pattern (34, 35). In somatic tissue, relaxation of imprinting occurs in certain pathological conditions (28, 36), and epigenetic heterogeneity at imprinted loci of autosomal chromosomes influences individual traits (37). The absence of *MeCP2_e2* correlated with up-regulation of *peg-1* expression, indicating a disturbance in regulation of downstream *MeCP2* gene targets. Although increased apoptosis in placenta could be used to explain the decreased viability of $X^{e2-}Y$ mice, this may also be interpreted as a way to eliminate functionally defective cells, thus contributing to the survival of some embryos.

The deleterious effects of *MeCP2* mutations have been viewed mostly in the context of somatic XCI patterns. A num-

ber of studies have addressed the contribution of XCI to the pathogenesis of *MeCP2* mutations (38, 39). It is suggested that XCI patterns may partly explain phenotypic variability in human RTT with *MeCP2* mutations (38) and in mouse RTT models (39). Our findings indicate that this is not the full picture and that paternal X chromosome inactivation in the extraembryonic lineage also contributes to the deleterious consequences of *MeCP2* mutations and, most likely, other X-linked gene mutations.

Recently, it has been reported that transgenic expression of either the *MeCP2_e1* or *MeCP2_e2* splice variant prevents the development of RTT-like neuronal phenotypic manifestations in a mouse model lacking *MeCP2*. This finding indicates that either *MeCP2* splice variant is sufficient to fulfill MeCP2 function in the mouse brain (40). Our findings reveal a novel mechanism for the pathogenesis of *MeCP2* mutations in extraembryonic tissue, wherein maternally inherited *MeCP2_e2* mutations result in placenta abnormalities that ultimately lead to a survival disadvantage for carriers of this mutant allele. Our study also provides an explanation for the absence of reports on *MeCP2_e2*-specific exon 2 mutations in RTT. It is conceivable that *MeCP2_e2* mutations in humans may result in a phenotype that evades a diagnosis of RTT. Moreover, the possible link between a novel genetic disorder characterized by reduced embryo viability and MeCP2 exon 2 mutations is a concept that merits further exploration. In summary, we have demonstrated that MeCP2_e2 is dispensable for RTT-associated neurological phenotypes. We have also discovered a novel requirement for MeCP2_e2 in placenta and embryo viability and have provided proof of existence of isoform-specific functions for two MeCP2 splicing variants.

*Acknowledgments—We thank Dr. S. Kudo for the MeCP2 antibody and helpful suggestions and S. Kumagai and N. Tomimatsu for help with some of the experiments.*

## REFERENCES


1. Amir, R. E., Van den Veyver, I. B., Wan, M., Tran, C. Q., Francke, U., and Zoghbi, H. Y. (1999) Rett syndrome is caused by mutations in X-linked MECP2, encoding methyl-CpG-binding protein 2. *Nat. Genet.* **23,** 185–188
2. Rett, A. (1966) [On an unusual brain atrophy syndrome in hyperammonemia in childhood]. *Wien Med. Wochenschr.* **116,** 723–726
3. Hagberg, B., Aicardi, J., Dias, K., and Ramos, O. (1983) A progressive syndrome of autism, dementia, ataxia, and loss of purposeful hand use in girls. Rett's syndrome. Report of 35 cases. *Ann. Neurol.* **14,** 471–479
4. Lewis, J. D., Meehan, R. R., Henzel, W. J., Maurer-Fogy, I., Jeppesen, P., Klein, F., and Bird, A. (1992) Purification, sequence, and cellular localization of a novel chromosomal protein that binds to methylated DNA. *Cell* **69,** 905–914
5. Meehan, R. R., Lewis, J. D., and Bird, A. P. (1992) Characterization of MeCP2, a vertebrate DNA-binding protein with affinity for methylated DNA. *Nucleic Acids Res.* **20,** 5085–5092
6. Nan, X., Ng, H. H., Johnson, C. A., Laherty, C. D., Turner, B. M., Eisenman, R. N., and Bird, A. (1998) Transcriptional repression by the methyl-CpG-binding protein MeCP2 involves a histone deacetylase complex. *Nature* **393,** 386–389
7. Jones, P. L., Veenstra, G. J., Wade, P. A., Vermaak, D., Kass, S. U., Landsberger, N., Strouboulis, J., and Wolffe, A.P. (1998) Methylated DNA and MeCP2 recruit histone deacetylase to repress transcription. *Nat. Genet.* **2,** 187–191
8. Harikrishnan, K. N., Chow, M. Z., Baker, E. K., Pal, S., Bassal, S., Brasacchio, D., Wang, L., Craig, J. M., Jones, P. L., Sif, S., and El-Osta, A. (2005) Brahma links the SWI/SNF chromatin-remodeling complex with MeCP2-dependent transcriptional silencing. *Nat. Genet.* **37,** 254–264
9. Kriaucionis, S., and Bird, A. (2004) The major form of MeCP2 has a novel N terminus generated by alternative splicing. *Nucleic Acids Res.* **32,** 1818–1823
10. Mnatzakanian, G. N., Lohi, H., Munteanu, I., Alfred, S. E., Yamada, T., MacLeod, P. J., Jones, J. R., Scherer, S. W., Schanen, N. C., Friez, M. J., Vincent, J. B., and Minassian, B. A. (2004) A previously unidentified MECP2 open reading frame defines a new protein isoform relevant to Rett syndrome. *Nat. Genet.* **36,** 339–341
11. Bienvenu, T., and Chelly, J. (2006) Molecular genetics of Rett syndrome. When DNA methylation goes unrecognized. *Nat. Rev. Genet.* **7,** 415–426
12. Guy, J., Hendrich, B., Holmes, M., Martin, J. E., and Bird, A. (2001) A mouse Mecp2-null mutation causes neurological symptoms that mimic Rett syndrome. *Nat. Genet.* **27,** 322–326
13. Chen, R. Z., Akbarian, S., Tudor, M., and Jaenisch, R. (2001) Deficiency of methyl-CpG binding protein-2 in CNS neurons results in a Rett-like phenotype in mice. *Nat. Genet.* **27,** 327–331
14. Fukuda, T., Itoh, M., Ichikawa, T., Washiyama, K., and Goto, Y. (2005) Delayed maturation of neuronal architecture and synaptogenesis in cerebral cortex of Mecp2-deficient mice. *J. Neuropathol. Exp. Neurol.* **64,** 537–544
15. Dragich, J. M., Kim, Y. H., Arnold, A. P., and Schanen, N. C. (2007) Differential distribution of the MeCP2 splice variants in the postnatal mouse brain. *J. Comp. Neurol.* **501,** 526–542
16. Chang, Y. S., Wang, L., Suh, Y. A., Mao, L., Karpen, S. J., Khuri, F. R., Hong, W. K., and Lee, H. Y. (2004) Mechanisms underlying lack of insulin-like growth factor-binding protein-3 expression in non-small-cell lung cancer. *Oncogene* **23,** 6569–6580
17. Itoh, M., Ide, S., Takashima, S., Kudo, S., Nomura, Y., Segawa, M., Kubota, T., Mori, H., Tanaka, S., Horie, H., Tanabe, Y., and Goto, Y. (2007) Methyl CpG-binding protein 2 (a mutation of which causes Rett syndrome) directly regulates insulin-like growth factor binding protein 3 in mouse and human brains. *J. Neuropathol. Exp. Neurol.* **66,** 117–123
18. Chen, W. G., Chang, Q., Lin, Y., Meissner, A., West, A. E., Griffith, E. C., Jaenisch, R., and Greenberg, M. E. (2003) Derepression of BDNF transcription involves calcium-dependent phosphorylation of MeCP2. *Science* **302,** 885–889
19. Mak, W., Nesterova, T. B., de Napoles, M., Appanah, R., Yamanaka, S., Otte, A. P., and Brockdorff, N. (2004) Reactivation of the paternal X chromosome in early mouse embryos. *Science* **303,** 666–669
20. Sado, T., and Ferguson-Smith, A. C. (2005) Imprinted X inactivation and reprogramming in the preimplantation mouse embryo. *Hum. Mol. Genet.* **14,** R59–64
21. Takagi, N., and Sasaki, M. (1975) Preferential inactivation of the paternally derived X chromosome in the extraembryonic membranes of the mouse. *Nature* **256,** 640–642
22. Harper, M. I., Fosten, M., and Monk, M. (1982) Preferential paternal X inactivation in extraembryonic tissues of early mouse embryos. *J. Embryol. Exp. Morphol.* **67,** 127–135
23. Obata, Y., Kaneko-Ishino, T., Koide, T., Takai, Y., Ueda, T., Domeki, I., Shiroishi, T., Ishino, F., and Kono, T. (1998) Disruption of primary imprinting during oocyte growth leads to the modified expression of imprinted genes during embryogenesis. *Development* **125,** 1553–1560
24. Coan, P. M., Burton, G. J., and Ferguson-Smith, A. C. (2005) Imprinted genes in the placenta. A review. *Placenta* **26,** S10–S20
25. Wu, X., Li, D. J., Yuan, M. M., Zhu, Y., and Wang, M. Y. (2004) The expression of CXCR4/CXCL12 in first-trimester human trophoblast cells. *Biol. Reprod.* **70,** 1877–1885
26. Mayer, W., Hemberger, M., Frank, H. G., Grümmer, R., Winterhager, E., Kaufmann, P., and Fundele, R. (2000) Expression of the imprinted genes MEST/Mest in human and murine placenta suggests a role in angiogenesis. *Dev. Dyn.* **217,** 1–10
27. Lefebvre, L., Viville, S., Barton, S. C., Ishino, F., Keverne, E. B., and Surani, M. A. (1998) Abnormal maternal behavior and growth retardation associated with loss of the imprinted gene Mest. *Nat. Genet.* **20,** 163–169

28. Looijenga, L. H., Gillis, A. J., Verkerk, A. J., van Putten, W. L., and Oosterhuis, J. W. (1999) Heterogeneous X inactivation in trophoblastic cells of human full-term female placentas. *Am. J. Hum. Genet.* **64,** 1445–1452
29. Beechey, C. V. (2000) Peg1/Mest locates distal to the currently defined imprinting region on mouse proximal chromosome 6 and identifies a new imprinting region affecting growth. *Cytogenet. Cell Genet.* **90,** 309–314
30. Nikonova, L., Koza, R. A., Mendoza, T., Chao, P. M., Curley, J. P., Kozak, L. P. (2008) Mesoderm-specific transcript is associated with fat mass expansion in response to a positive energy balance. *FASEB J.* **22,** 3925–3937
31. Lee, K. Y., Jeong, J. W., Tsai, S. Y., Lydon, J. P., and DeMayo, F. J. (2007) Mouse models of implantation. *Trends Endcrinol. Metab.* **18,** 234–239
32. Watson, E. D., and Cross, J. C. (2005) Development of structures and transport functions in the mouse placenta. *Physiology* **20,** 180–193
33. Chaddha, V., Viero, S., Huppertz, B., and Kingdom, J. (2004) Developmental biology of the placenta and the origins of placental insufficiency. *Semin. Fetal Neonatal Med.* **9,** 357–369
34. Migeon, B. R., Wolf, S. F., Axelman, J., Kaslow, D. C., and Schmidt, M. (1985) Incomplete X chromosome dosage compensation in chorionic villi of human placenta. *Proc. Natl. Acad. Sci. U.S.A.* **82,** 3390–3394
35. Coutinho-Camillo, C. M., Brentani, M. M., Butugan, O., Torloni, H., and Nagai, M. A. (2003) Relaxation of imprinting of IGFII gene in juvenile nasopharyngeal angiofibromas. *Diagn. Mol. Pathol.* **12,** 57–62
36. Sakatani, T., Wei, M., Katoh, M., Okita, C., Wada, D., Mitsuya, K., Meguro, M., Ikeguchi, M., Ito, H., Tycko, B., and Oshimura, M. (2001) Epigenetic heterogeneity at imprinted loci in normal populations. *Biochem. Biophys. Res. Commun.* **283,** 1124–1130
37. Bourdon, V., Philippe, C., Martin, D., Verloès, A., Grandemenge, A., and Jonveaux, P. (2003) MECP2 mutations or polymorphisms in mentally retarded boys. Diagnostic implications. *Mol. Diagn.* **7,** 3–7
38. Shahbazian, M. D., Sun, Y., and Zoghbi, H. Y. (2002) Balanced X chromosome inactivation patterns in the Rett syndrome brain. *Am. J. Med. Genet.* **111,** 164–168
39. Young, J. I., and Zoghbi, H. Y. (2004) X-chromosome inactivation patterns are unbalanced and affect the phenotypic outcome in a mouse model of rett syndrome. *Am. J. Hum. Genet.* **74,** 511–520
40. Kerr, B., Soto, C. J., Saez, M., Abrams, A., Walz, K., and Young, J. I. (2012) Transgenic complementation of MeCP2 deficiency. Phenotypic rescue of Mecp2-null mice by isoform-specific transgenes. *Eur. J. Hum. Genet.* **20,** 69–76

# Alterations of Gene Expression and Glutamate Clearance in Astrocytes Derived from an MeCP2-Null Mouse Model of Rett Syndrome

**Yasunori Okabe[1,2], Tomoyuki Takahashi[1,3]*, Chiaki Mitsumasu[1,3], Ken-ichiro Kosai[1,3,4], Eiichiro Tanaka[1,2], Toyojiro Matsuishi[1,3]**

**1** Division of Gene Therapy and Regenerative Medicine, Cognitive and Molecular Research Institute of Brain Diseases, Kurume University, Kurume, Japan, **2** Department of Physiology, Kurume University of Medicine, Kurume, Japan, **3** Department of Pediatrics, Kurume University of Medicine, Kurume, Japan, **4** Department of Gene Therapy and Regenerative Medicine, Advanced Therapeutics Course, Kagoshima University Graduate School of Medical and Dental Sciences, Kagoshima, Japan

## Abstract

Rett syndrome (RTT) is a neurodevelopmetal disorder associated with mutations in the methyl-CpG–binding protein 2 (MeCP2) gene. MeCP2-deficient mice recapitulate the neurological degeneration observed in RTT patients. Recent studies indicated a role of not only neurons but also glial cells in neuronal dysfunction in RTT. We cultured astrocytes from MeCP2-null mouse brain and examined astroglial gene expression, growth rate, cytotoxic effects, and glutamate (Glu) clearance. Semi-quantitative RT-PCR analysis revealed that expression of astroglial marker genes, including GFAP and S100β, was significantly higher in MeCP2-null astrocytes than in control astrocytes. Loss of MeCP2 did not affect astroglial cell morphology, growth, or cytotoxic effects, but did alter Glu clearance in astrocytes. When high extracellular Glu was added to the astrocyte cultures and incubated, a time-dependent decrease of extracellular Glu concentration occurred due to Glu clearance by astrocytes. Although the shapes of the profiles of Glu concentration versus time for each strain of astrocytes were grossly similar, Glu concentration in the medium of MeCP2-null astrocytes were lower than those of control astrocytes at 12 and 18 h. In addition, MeCP2 deficiency impaired downregulation of excitatory amino acid transporter 1 and 2 (EAAT1/2) transcripts, but not induction of glutamine synthetase (GS) transcripts, upon high Glu exposure. In contrast, GS protein was significantly higher in MeCP2-null astrocytes than in control astrocytes. These findings suggest that MeCP2 affects astroglial genes expression in cultured astrocytes, and that abnormal Glu clearance in MeCP2-deficient astrocytes may influence the onset and progression of RTT.

**Citation:** Okabe Y, Takahashi T, Mitsumasu C, Kosai K-i, Tanaka E, et al. (2012) Alterations of Gene Expression and Glutamate Clearance in Astrocytes Derived from an MeCP2-Null Mouse Model of Rett Syndrome. PLoS ONE 7(4): e35354. doi:10.1371/journal.pone.0035354

**Editor:** Nicoletta Landsberger, University of Insubria, Italy

**Received** October 26, 2011; **Accepted** March 14, 2012; **Published** April 20, 2012



**Funding:** This work was supported in part by a Grant-in-Aid for Scientific Research (C) and a Grant-in-Aid for Young Scientists (B) from the Japan Society for the Promotion of Science. The funders had no role in study design, data collection and analysis, decision to publish, or preparation of the manuscript.

**Competing Interests:** The authors have declared that no competing interests exist.

* E-mail: takahashi_tomoyuki@kurume-u.ac.jp

## Introduction

Rett syndrome (RTT) is a neurodevelopmetal disorder that affects one in 15,000 female births, and represents a leading cause of mental retardation and autistic behavior in girls [1,2]. Mutations in the methyl-CpG–binding protein 2 (MeCP2) gene, located in Xq28, have been identified as the cause for the majority of clinical RTT cases [3]. Knockout mouse models with disrupted MeCP2 function mimic many key clinical features of RTT, including normal early postnatal life followed by developmental regression that results in motor impairment, irregular breathing, and early mortality [4,5,6]. MeCP2 dysfunction may thus disrupt the normal developmental or/and physiological program of gene expression, but it remains unclear how this might result in a predominantly neurological phenotype.

In several RTT mouse models, a conditional knockout that is specific to neural stem/progenitor cells or postmitotic neurons results in a phenotype that is similar to the ubiquitous knockout, suggesting that MeCP2 dysfunction in the brain and specifically in neurons underlies RTT [1,6,7]. Recent studies have demonstrated that mice born with RTT can be rescued by reactivation of neuronal MeCP2 expression, suggesting that the neuronal damage can be reversed [1,6]. In addition, several studies using in vitro cell culture systems also indicate that MeCP2 may play a role in processes of neuronal maturation including dendritic growth, synaptogenesis, and electrophysiological responses [1,7]. These data support the idea that MeCP2 deficiency in neurons is sufficient to cause an RTT-like phenotype. However, emerging evidence now indicates that MeCP2 deficiency in glia may also have a profound impact on brain function [8,9,10,11,12,13]. Brain magnetic resonance (MR) studies in MeCP2-deficient mice demonstrated that metabolism in both neurons and glia is affected [8]. Furthermore, in vitro co-culture studies have shown that MeCP2-deficient astroglia non-cell-autonomously affect neuronal dendritic growth [9,10]. In addition, MeCP2-deficient microglia cause dendritic and synaptic damage mediated by elevated glutamate (Glu) release [11]. Very recent studies have indicated that re-expression of MeCP2 in astrocytes of MeCP2-deficient mice significantly improves locomotion, anxiety levels, breathing patterns, and average lifespan, suggesting that astrocyte dysfunc-

tion may be involved in the neuropathology and characteristic phenotypic regression of RTT [13].

Astrocytes regulate the extracellular ion content of the central nervous systems (CNS); they also regulate neuron function, via production of cytokines, and synaptic function, by secreting neurotransmitters at synapses [14,15]. Moreover, a major function of astrocytes is efficient removal of Glu from the extracellular space, a process that is instrumental in maintaining normal interstitial levels of this neurotransmitter [16]. Glu is a major excitatory amino acid; excess Glu causes the degeneration of neurons and/or seizures observed in various CNS diseases [14,17]. RTT is also associated with abnormalities in Glu metabolism, but these findings are controversial due to the limitations of the experimental strategies used. Two studies have demonstrated that Glu is elevated in the cerebrospinal fluid (CSF) of RTT patients [18,19]. MR spectroscopy in RTT patients also revealed elevations of the Glu and Gln peak [20,21]. On the other hand, an animal MR study reported that the levels of Glu and Gln were decreased in a mouse model of RTT [8]. A more recent study indicated that MeCP2-null mice have reduced levels of Glu, but elevated levels of Gln, relative to their wild-type littermates [22]. Another study reported increased Gln levels and Gln/Glu ratios in Mecp2 mutant mice, but no decreases in Glu levels [23]. Although these in vivo studies have explored the hypothesis that the Glu metabolic systems might be altered in RTT, no solid conclusions have yet been reached [24,25].

In this study, we investigated the contribution of MeCP2 to the physiological function of astrocytes. Our studies demonstrate that MeCP2 is not essential for the growth and survival of astrocytes, but is involved in astrocytic Glu metabolism via the regulation of astroglial gene expression.

## Results

### Characterization of MeCP2-null astrocytes

It was recently reported that MeCP2 is normally present not only in neurons but also in glia, including astrocytes, oligodendrocytes, and microglia [9,10,11]. To determine the roles of MeCP2 in astrocytes, we cultured cerebral cortex astrocytes from both wild-type ($MeCP2^{+/y}$) and MeCP2-null ($MeCP2^{-/y}$) mouse brains (Fig. 1). MeCP2-null astrocytes exhibited a large, flattened, polygonal shape identical to that of the wild-type astrocytes, suggesting that normal patterns of cellular recognition and contact were present. Semi-quantitative RT-PCR using primer sets that specifically amplify two splice variants, Mecp2 e1 and e2, showed that control astrocytes expressed Mecp2 e1 and e2, whereas neither Mecp2 variant was detectable in MeCP2-null astrocytes (Fig. 1A). We further confirmed expression of MeCP2 by immunocytochemical staining of astrocytes. In control samples, almost all GFAP-positive cells exhibited clear nuclear MeCP2 immunoreactivity in astrocytes, but no immunoreactivity was observed in MeCP2-null astrocytes (Fig. 1B).

MeCP2 has been reported to be involved in regulation of astroglial gene expression [26,27]. Consistent with this, GFAP levels were significantly higher in MeCP2-null astrocytes (Fig. 1A). Similarly, the expression of S100β, another astrocyte maturation marker, was significantly upregulated by MeCP2 deficiency (fold change of control = 1.0, GFAP: 2.195±0.504, n = 4 each, $p<0.05$; S100β: 2.779±0.329, n = 4 each, $p<0.01$). These results show that MeCP2 deficiency upregulates astroglial gene expression in astrocytes.

To compare the growth of the wild-type and MeCP2-null astrocytes, we counted total cell number at each passage (Fig. 2A). As passage number increased, the cell growth rate decreased dramatically for both types of astrocytes, ultimately culminating in senescence. There was no significant difference in growth rate between the control and MeCP2-null astrocyte cultures. We then measured astrocyte proliferation via BrdU incorporation assay (Fig. 2B and Fig. S1). After 2 h of BrdU treatment, the proportions of BrdU-incorporating cells were similar in the control and MeCP2-null astrocytes (6.635±1.655% in control versus 6.774±2.272% in MeCP2-null astrocytes, n = 4 each, p = 0.962). These results suggest that the absence of MeCP2 did not affect the proliferation of astrocytes in our culture condition.

We also tested the cytotoxic effects of hydrogen peroxide ($H_2O_2$), ammonium chloride ($NH_4Cl$), and glutamate (Glu), on astrocytes in our culture (Fig. 2C–E). In cultures derived from both wild-type and MeCP2-null strains, cell viability decreased with increasing concentrations of $H_2O_2$ and $NH_4Cl$. In contrast, in our culture conditions, we observed virtually 100% viability of both the control and MeCP2-null astrocytes after 24 h incubation with 10 mM Glu. Glu-induced gliotoxic effects have been previously reported by Chen et al. (2000), and are probably due to distinct differences in culture conditions, specifically the presence of glucose [28]. These results showed that $H_2O_2$ and $NH_4Cl$ had a similar effect in both strains of astrocytes. There was no significant difference in viability between the control and MeCP2-null astrocyte cultures, indicating that MeCP2 deficiency did not affect astrocyte viability upon treatment with $H_2O_2$ and $NH_4Cl$.

### Effects of glutamate on glutamate transporters and glutamine synthetase transcripts in MeCP2-null astrocytes

High extracellular Glu interferes with the expression of the astrocyte transporter subtypes, excitatory amino acid transporter 1(EAAT1)/glutamate/aspartate transporter (GLAST) and EAAT2/glutamate transporter-1 (GLT-1) [16,29]. To explore the effects of Glu on the expression of Glu transporter genes in cultured astrocytes from wild-type and MeCP2-null mouse brains, we asked whether treatment with 1.0 mM Glu altered expression of EAAT1 and EAAT2 mRNA, using a semi-quantitative RT-PCR assay (Fig. 3). EAAT1 and EAAT2 mRNA were expressed in both wild-type and MeCP2-null astrocytes, and were slightly higher in controls than in MeCP2-null astrocytes. Both EAAT1 and EAAT2 mRNA levels were altered in the control astrocytes after treatment with 1.0 mM Glu. EAAT1 mRNA levels decreased significantly in the wild-type astrocytes, both 12 h and 24 h after treatment with Glu (Fig. 3A). In contrast, EAAT1 decreased significantly in the MeCP2-null astrocytes, at 12 h but not 24 h after treatment. As with EAAT1, EAAT2 mRNA levels also decreased significantly in the control astrocytes, both 12 h and 24 h after treatment (Fig. 3B). However, EAAT2 decreased significantly in MeCP2-null astrocytes, 24 h but not 12 h after treatment. In addition, the effects of Glu on EAAT1 and EAAT2 relative fold expression at 12 h were altered in the MeCP2-null astrocytes (Fig. 3D: EAAT1; 0.618±0.033 in control versus 0.758±0.049 in MeCP2-null astrocytes, n = 10 each, $p<0.05$; Fig. 3E: EAAT2; 0.794±0.055 in control versus 0.964±0.048 in MeCP2-null astrocytes, n = 8 each, $p<0.05$). These results suggest that the loss of MeCP2 leads to transcriptional dysregulation of these genes, either directly or indirectly.

One important enzyme that plays a role in the Glu metabolic pathway is glutamine synthetase (GS) [17,29]. GS is mainly located in astrocytes; cultured astrocytes response to Glu with increased GS expression [17,29]. Consistent with this, 1.0 mM Glu treatment stimulated GS mRNA expression in both the wild-type and MeCP2-null astrocytes about 1.2-fold after 12 h but not 24 h (Fig. 3C). In addition, MeCP2 deficiency did not modify the

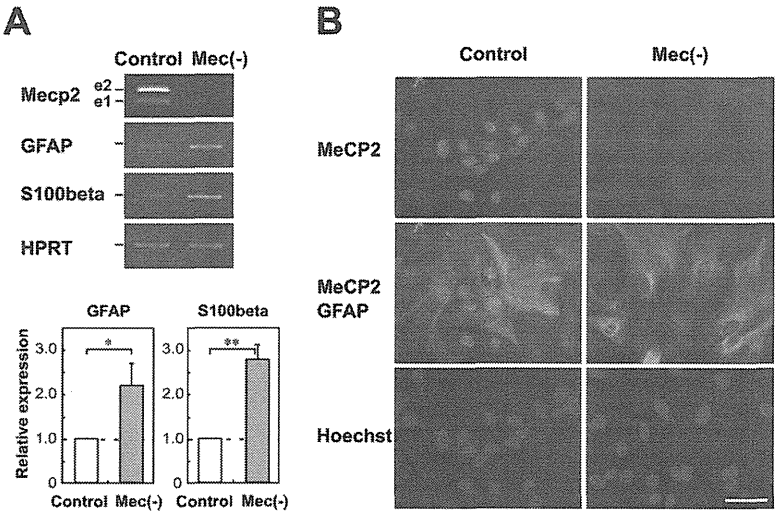


**Figure 1. Characterization of assay cultures. A.** Expression of astroglial genes in primary cultured cortical astrocytes. Semi-quantitative RT-PCR analysis of Mecp2 and astroglial genes was performed in wild-type (white column) and MeCP2-null (gray column) astrocytes. Mecp2 e1 and e2 were detectable in the wild-type astrocytes. The lower graphs show that the GFAP/HPRT or S100β/HPRT expression ratio in each genotype was normalized against the level in control astrocytes. Bars represent the means ± standard errors (SE) of samples from three independent experiments (*$p<0.05$). The expression of astroglial markers was significantly upregulated by MeCP2 deficiency. **B.** Expression of MeCP2 in the primary cultured cortical astrocytes. The astrocytes were immunostained with MeCP2 (green) and GFAP (red) as glial-specific astrocytic markers. Scale bars indicate 50 μm.
doi:10.1371/journal.pone.0035354.g001

effects of Glu on GS mRNA relative fold expression in cultured astrocytes (Fig. 3F, 1.245±0.054 in control versus 1.265±0.093 in MeCP2-null astrocytes, n = 6 each, p = 0.859). These results suggested that MeCP2 did not modify the expression of GS in the cultured astrocytes. Overall, the expression levels of GS mRNA did not differ between both strains of astrocytes following treatment with Glu.

## Comparison of glutamate clearance between wild-type and MeCP2-null astrocytes

Because MeCP2 contributed to the transcriptional regulation of Glu metabolism-related genes in our culture systems, we next compared the Glu clearance capability of the wild-type and MeCP2-null astrocytes (Fig. 4A). The cell culture supernatants in both astrocyte cultures were collected at 3–24 h post incubation in culture media containing 1.0 mM Glu. After incubation in culture medium containing Glu, we identified a time-dependent reduction in Glu over 24 h of incubation in both strains of astrocytes. Although the shapes of the profiles of Glu concentration versus time for each strain of astrocytes were grossly similar, Glu concentration in the medium of MeCP2-null astrocytes were lower than those of control astrocytes at 12 and 18 h (12 h: control, 0.513±0.052 mM versus MeCP2-null, 0.395±0.022 mM, $p<0.05$; 18 h: control, 0.368±0.029 mM versus MeCP2-null, 0.125±0.007 mM, $p<0.01$, n = 6 each, Fig. 4A). The differences in Glu clearance were not due to changes in cell death of control astrocytes upon application of Glu (Fig. 2E). This indicates that Glu clearance by MeCP2-null astrocytes was more efficient than by control astrocytes.

The Glu transporters EAAT1 and EAAT2 are located primarily on astrocytes and are critical in maintaining extracellular Glu at safe levels [16]. Threo-beta-benzyloxyaspartate (TBOA) is a broad-spectrum glutamate transporter antagonist, affecting EAAT1 and EAAT2 [30]. UCPH-101 (2-amino-4-(4-methoxyphenyl)-7-(naphthalen-1-yl)-5-oxo-5,6,7,8-tetrahydro-4H-chromene-3-carbonitrile) and dihydrokainate (DHKA) are selective inhibitors for EAAT1 and EAAT2, respectively [30,31]. To investigate the functional Glu transporters in our astrocyte cultures, we analyzed three Glu transporter blockers (TBOA, UCPH-101, or DHKA) for their ability to alter the effects of Glu clearance (Fig. 4B–D). Glu clearance by the wild-type astrocytes was partially blocked by addition of TBOA and UCPH-101, but not DHKA. This suggests that EAAT1, but not EAAT2, plays a major role in Glu clearance under our astroglial culture conditions.

## Effects of glutamate on glutamine synthetase and EAAT1 protein in MeCP2-null astrocytes

The initial set of experiments aimed to determine whether Glu modulate the translation of GS and EAAT1 protein (Fig. 5 and Fig. S2). GS protein was expressed in both wild-type and MeCP2-null astrocytes, and was significantly more abundant in MeCP2-null astrocytes (Fig. 5B: fold change of control = 1.0, 2.631±0.368, $p<0.01$). After 12 h exposure to 0.01–1.0 mM Glu, wild-type astrocytes exhibited a dose-dependent increase in GS protein levels (about 6-fold in 1.0 mM Glu treatment). Similar to its effect on the wild-type astrocytes, in the MeCP2-null astrocytes Glu exposure dose-dependently increased GS protein levels relative to untreated astrocytes (Fig. S2). We then examined the effect of 1.0 mM Glu on levels of GS protein, over a time course (Fig. 5A). GS expression was highest after 12 h exposure to 1.0 mM Glu, decreasing slightly by 24 h in both wild-type and MeCP2-null astrocytes. Densitometric analysis of the bands in three independent experiments demonstrated that GS protein in MeCP2-null astrocyte cultures was higher than in wild-type astrocytes, 12 h but not 24 h after treatment (Fig. 5B: fold change of control = 1.0, at 12 h: 1.421±0.139, $p<0.05$; at 24 h: 1.131±0.130, p = 0.354, n = 4 each). These results indicated that MeCP2 deficiency caused higher expression of GS protein in cultured astrocytes.

We also asked whether treatment with 1.0 mM Glu altered expression of EAAT1 protein. EAAT1 protein was expressed in

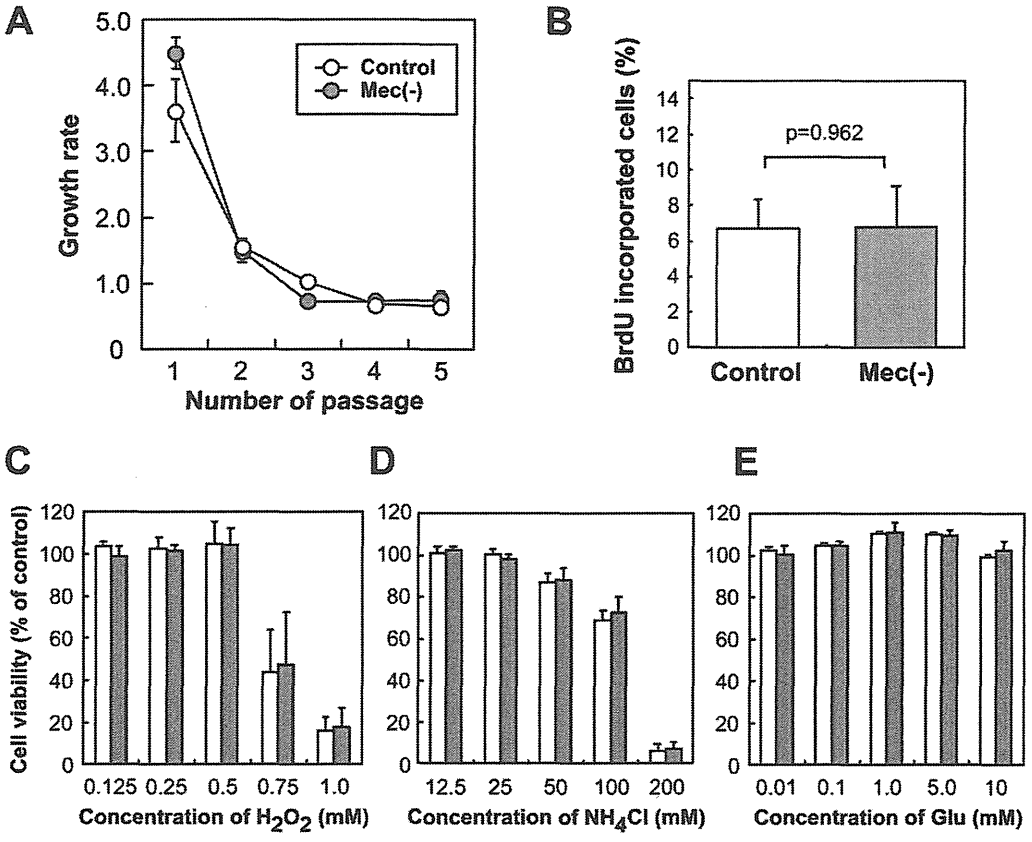


**Figure 2. Cell growth and viability. A.** Comparison of cell growth in wild-type and MeCP2-deficient astrocytes. As passage number increased, cell growth rate decreased dramatically in both strains of astrocytes. There was no significant difference in growth rate between the control and MeCP2-null astrocyte cultures. **B.** Quantification of BrdU-incorporating cells in control and MeCP2-null astrocytes. Astrocytes were cultured for 24 h and incubated with BrdU for 2 h. The graph shows the percentage of BrdU-incorporating cells in the control (white column) and MeCP2-deficient (gray column) astrocytes 2 h after BrdU exposure. The number of BrdU-incorporating cells is expressed as a percentage of the total number of Hoechst-stained cells (Fig. S1). Bars represent the means ± SE of the samples from four independent experiments. The ratio of BrdU-incorporating cells is similar in astrocytes taken from both control and MeCP2-null strains. **C–E.** Comparison of effects of various neurotoxins (**C,** $H_2O_2$; **D,** $NH_4Cl$; **E,** Glutamate) on control and MeCP2-null astrocytes. The graph shows the percentage of viability in the control (white column) and MeCP2-deficient (gray column) astrocytes after neurotoxin treatment at the indicated concentrations. Bars represent the means ± SE of samples from three independent experiments. The glial cultures showed no difference in viability between the control and MeCP2-null strains.
doi:10.1371/journal.pone.0035354.g002

both wild-type and MeCP2-null astrocytes, at levels that were similar in controls and MeCP2-null astrocytes. EAAT1 protein levels were altered in the wild-type astrocytes after treatment with 1.0 mM Glu. EAAT1 protein levels decreased significantly in the wild-type astrocytes, 24 h but not 12 h after treatment (Fig. 5C). In contrast, EAAT1 did not decrease in the MeCP2-null astrocytes, either 12 h or 24 h after treatment. In addition, the relative expression levels of EAAT1 24 h after treatment were lower in the wild-type than in the MeCP2-null culture, although the difference was not statistically significant (Fig. 5D: 12 h; 1.102±0.169 in control versus 1.096±0.142 in MeCP2-null astrocytes, n = 6 each, p = 0.979, 24 h; 0.456±0.123 in control versus 0.901±0.172 in MeCP2-null astrocytes, n = 5 each, p = 0.068). These results suggest that MeCP2 deficiency affects the expression of GS and EAAT1 protein, and that accelerated Glu clearance may result from dysregulation of GS and EAAT1 protein in MeCP2-null astrocytes.

## Discussion

Recent studies suggest that glia, as well as neurons, cause neuronal dysfunction in RTT via non-cell-autonomous effects. Here, we have demonstrated that MeCP2 regulates the expression of astroglial marker transcripts, including GFAP and S100β in cultured astrocytes. In addition, MeCP2 is not essential for the cell morphology, growth, or viability; rather, it is involved in Glu clearance through the regulation of Glu transporters and GS in astrocytes. Altered astroglial gene expression and abnormal Glu clearance by MeCP2-null astrocytes may underlie the pathogenesis of RTT.

In this study, MeCP2-null astrocytes exhibited significantly higher transcripts corresponding to astroglial markers, including GFAP and S100β. Consistent with this, transcription of several astrocytic genes, including GFAP, is upregulated in RTT patients [26,32]. Indeed, MeCP2 binds to a highly methylated region in the GFAP and S100β in neuroepithlial cells [27,33]; ectopic

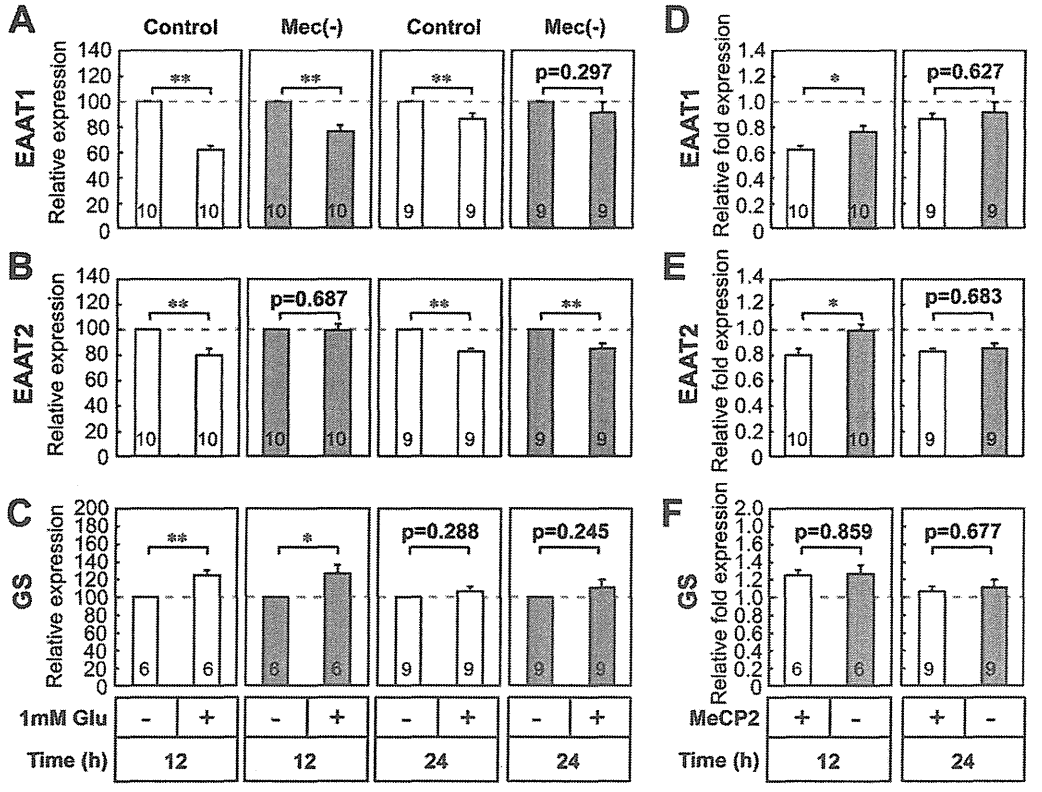


**Figure 3. Effect of glutamate on glutamine synthetase and glutamate transporter gene expression in MeCP2-null astrocytes. A–C.** Effects of Glu on Glu clearance-related genes in wild-type (white column) and MeCP2-null (gray column) astrocytes. Semi-quantitative RT-PCR analysis of Glu clearance-related genes, EAAT1 (**A**), EAAT2 (**B**), and GS (**C**), was performed in the control and MeCP2-null astrocytes 12 or 24 h after treatment with 1.0 mM Glu. The bands corresponding to PCR products were quantified by densitometry, normalized against HPRT levels, and expressed as % of controls (equals 100%). Bars represent the means ± SE of samples from 3–4 independent experiments (*$p<0.05$, **$p<0.01$). **D–F.** Comparison of the effects of Glu on EAAT1, EAAT2 or GS expression in the control and MeCP2-null astrocytes. The ratio of EAAT1/HPRT (**D**), EAAT2/HPRT (**E**) or GS/HPRT (**F**) in each treatment group was normalized against that of the non-treated astrocytes from each group. Bars represent the means ± SE of samples from 3–5 independent experiments (*$p<0.05$). Numbers in each column indicate the total number of samples analyzed.
doi:10.1371/journal.pone.0035354.g003

overexpression of MeCP2 inhibited the differentiation of neuroepithelial cells into GFAP-positive glial cells [34]. Our recent study in RTT-model ES cells also demonstrated that MeCP2 is involved in gliogenesis during neural differentiation via inhibition of GFAP expression [12]. Therefore, MeCP2 may be involved not only in the suppression of astroglial genes in neuroepithelial cells/neurons during neurogenesis, but also in the physiological regulation of astroglial gene expression in astrocytes.

We also demonstrated that MeCP2 is not essential for cell growth or cell viability in in vitro models of astrocyte injury, such as $H_2O_2$ oxidative stress and ammonia neurotoxicity. On the other hand, it has been reported that MeCP2 is involved in regulating astrocyte proliferation, and are probably due to distinct differences in culture conditions, specifically the presence of serum [10]. Consistent with these results, obvious neuronal and glial degeneration had not been observed in RTT [6,35]. These observations suggest that RTT is not caused by reduced cell numbers, but rather by dysfunction of specific cell types in the brain.

The regulation of Glu levels in the brain is an important component of plasticity at glutamatergic synapses, and of neuronal damage via excessive activation of Glu receptors [15,16]. Astrocytic uptake of Glu, followed by conversion of Glu to Glutamine (Gln), is the predominant mechanism of inactivation of Glu once it has been released in the synaptic cleft. This uptake involves two transporters, EAAT1/GLAST and EAAT2/GLT-1 [16]. Increases in extracellular Glu, present in many brain injuries, are sufficient to modulate the expression of Glu transporters and GS [16,29]. Furthermore, application of 0.5–1.0 mM Glu to cultured cortical astrocytes causes a decline in EAAT1/GLAST and EAAT2/GLT-1 expression [29]. Our present studies reveal that 1.0 mM extracellular Glu is sufficient to inhibit astroglial Glu transporter expression and to stimulate GS expression in control astrocytes. However, such regulatory influences on Glu transporters are impaired by MeCP2 deficiency. Therefore, MeCP2 may regulate the expression of Glu transporters under physiological conditions. Currently, little is known about the promoter regions of the main Glu transporters [36,37]. Promoter analysis in each gene may help to elucidate the complex regulations of astroglial genes by MeCP2.

On the other hand, in our culture conditions, MeCP2 deficiency did not impair the expression of GS transcripts in cultured astrocytes, but did affect the expression of GS protein. A very recent study has shown that defects in the AKT/mTOR pathway

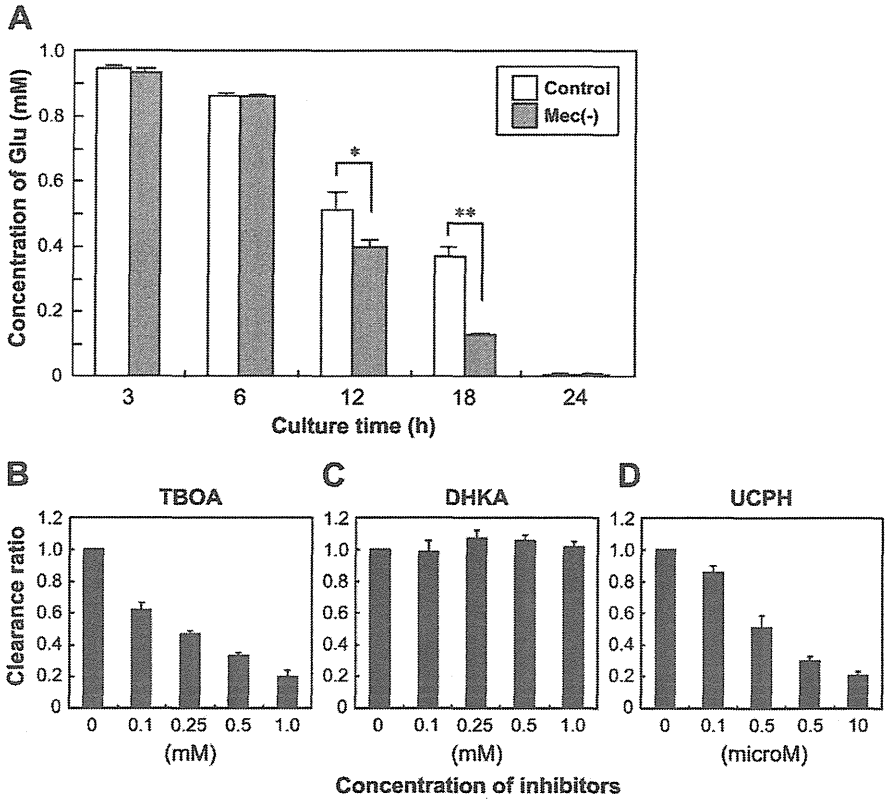


**Figure 4. Comparison of glutamate clearance in wild-type and MeCP2-null astrocytes. A.** Time-dependent reduction of extracelluar Glu concentration in wild-type (white column) and MeCP2-null (gray column) astrocyte cultures. After treatment with 1.0 mM Glu, culture supernatant was collected at the indicated times for the determination of Glu concentration. The graph shows the concentration of Glu in control and MeCP2-null astrocyte culture medium. Bars represent the means ± SE of samples from three independent experiments (*$p<0.05$). **B–D.** Effects of inhibitors of glutamate transporters (**B,** TBOA; **C,** DHKA; **D,** UCPH) on Glu clearance. Astrocytes were exposed to the indicated concentration of Glu transporter inhibitors, and then 0.1 mM Glu was added; culture supernatant was collected for the determination of Glu concentration at 2 h. The graphs show the clearance ratio upon treatment with each inhibitor. The clearance ratio in the indicated concentration groups was expressed by defining the control level (no inhibitor) as 1.0. Bars represent the means ± SE of samples from three independent experiments.
doi:10.1371/journal.pone.0035354.g004

are responsible for altered translational control in MeCP2 mutant neuron [38]. These findings suggest that a deficit in protein synthesis and/or turnover in the MeCP2-null astrocytes might influence the final levels of GS protein. Further studies are necessary to investigate whether MeCP2 deficiency impairs the synthesis and turnover of proteins in RTT.

The most important finding in this study was that MeCP2 deficiency in astrocytes accelerates Glu clearance. Consistent with this, RTT is associated with abnormalities in the Glu metabolism [24]. Some studies have demonstrated increases in Glu levels in the cerebrospinal fluid (CSF) of human RTT patients [18,19]. On the other hand, in animal studies there have been instances of decreased Glu levels and/or Glu/Gln ratios, as determined by in MR spectroscopy [8,21,22,23]. Furthermore, MeCP2-deficient microglia release an abnormally high level of Glu, causing excitotoxicity that may contribute to dendritic and synaptic abnormalities in RTT [11]. These results clearly suggest that MeCP2 has the potential to regulate Glu levels in the brain under certain circumstances. Glu levels are altered in the RTT brain, but the mechanisms responsible for the changes in Glu metabolism are unknown. In light of our findings, we speculate that abnormal expression of Glu transporters and GS resulting from MeCP2 deficiency could lead to abnormal Glu clearance in astrocytes and in turn to altered levels of Glu in RTT brain. Additional studies are needed to determine the mechanisms underlying changes in Glu levels and Glu metabolism, and their role in the RTT brain.

In conclusion, MeCP2 modulates Glu clearance through the regulation of astroglial genes in astrocytes. This study suggests a novel role for MeCP2 in astrocyte function; these findings may be useful in exploration of a new approach for preventing the neurological dysfunctions associated with RTT.

## Materials and Methods

### Cell culture

For each experiment, primary cultures were generated from individual MeCP2-null neonates and their wild-type littermates; tail snips from each neonate were obtained for genotyping, as described below. Enriched cultures of GFAP-expressing astroglial cells, which are virtually free of neurons and microglial cells, were established from the cerebral hemispheres of postnatal day (P) 0 to P1 newborn mice, as previously described [29]. In brief, pieces of dissected tissue were trypsinized (0.05%) for 10 min in $Ca_2^+$- and $Mg_2^+$-free phosphate-buffered saline (PBS) supplemented with

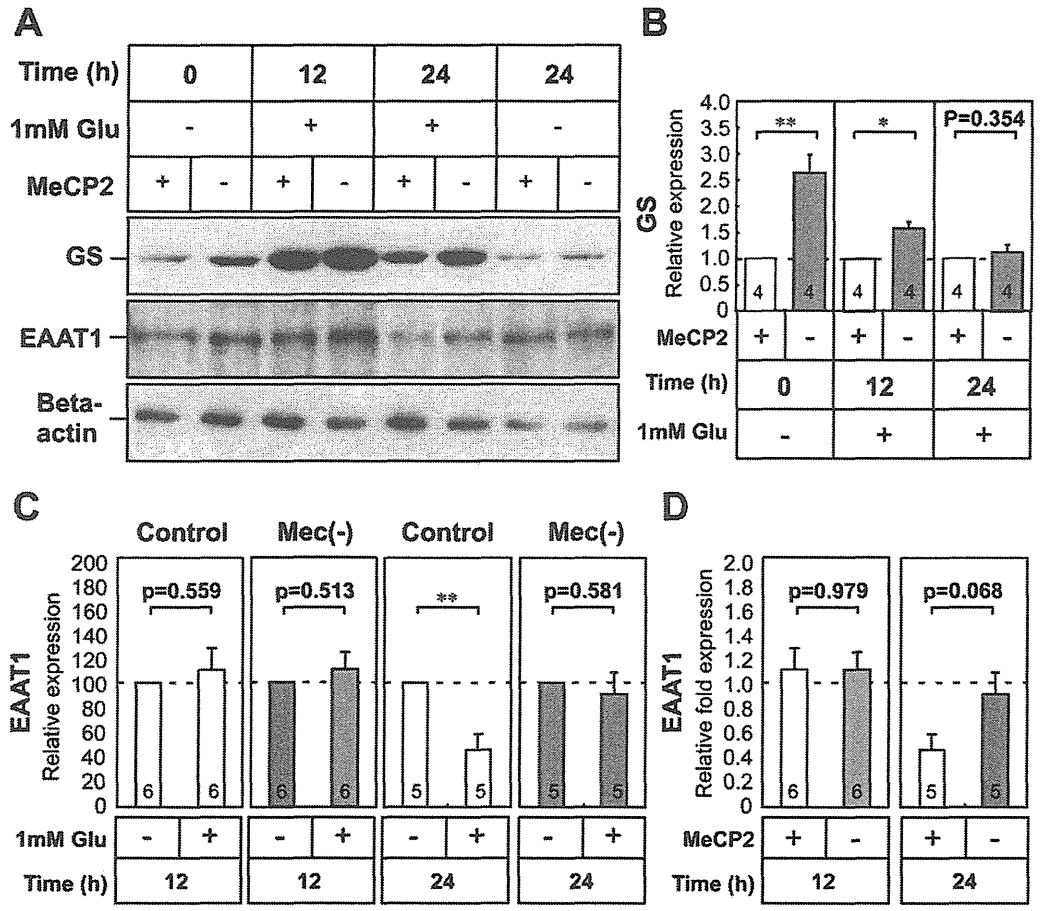


**Figure 5. Effect of glutamate on glutamine synthetase and EAAT1 protein expression in MeCP2-null astrocytes. A.** Time-dependent expression of GS and EAAT1 proteins in wild-type and MeCP2-deficient astrocyte cultures. Astrocytes were treated with 1.0 mM Glu for 24 h, and subsequently analyzed for expression of GS and EAAT1 by Western blot analysis. Beta-actin protein levels were analyzed in the same way, as an internal control. **B.** The immunoreactive GS protein bands were quantified by densitometry, normalized against β-actin levels, and expressed as fold change relative to the controls (equals 1.0). Bars represent the means ± SE of samples from three independent experiments (*$p<0.05$, **$p<0.01$). Numbers in each column indicate the total number of samples analyzed. **C.** The immunoreactive EAAT1 protein bands were quantified by densitometry, normalized against β-actin levels, and expressed as % of controls (equals 100%). Bars represent the means ± SE of samples from three independent experiments (**$p<0.01$). **D.** Comparison of the effects of Glu on EAAT1 expression in wild-type and MeCP2-null astrocytes. The ratio of EAAT1/β-actin in each treatment group was normalized against that of the non-treated astrocytes from each group. Bars represent the means ± SE of samples from three independent experiments. Numbers in each column indicate the total number of samples analyzed.
doi:10.1371/journal.pone.0035354.g005

0.02% EDTA. Tissue samples were subsequently dissociated in Hank's balanced salt solution (HBSS) containing 15% fetal calf serum (FCS; F2442, Sigma-Aldrich, Inc., St. Louis, MO, USA) by trituration though 10-ml plastic pipettes. Cells were pelleted at 100×g for 5 min, resuspended in Dulbecco's modified Eagle's medium (D-MEM; Wako Pure Chemical Industries, Ltd., Osaka, Japan) containing 15% FCS, and seeded into 100-mm culture dishes previously coated with poly-D-lysine (0.1 mg/ml; Wako Pure Chemical Industries, Ltd., Osaka, Japan). Upon reaching confluency, cells were trypsinized and replated. Cells were used after the third passage (P3) in all experiments, and were seeded at $3\times10^4$ cells/cm$^2$ in 6-well plate dishes or 35-mm culture dishes. Cultures were assayed by immunochemical analysis using antibodies against GFAP, MAP2, and CD11b in order to determine the degree of enrichment; the astrocyte cultures were nearly pure without contamination of microglia and neurons (Fig. S3 and Information S1).

## Cell growth and bromo-2′-deoxyuridine (BrdU) uptake assay

To determine growth rate, cells were plated at $2\times10^5$ cells/dish in 35-mm dishes. At each passage, three dishes per cell line were harvested by trypsinization, and cell numbers were determined using a hemocytometer. Growth rate was expressed as the number of harvested cells divided by the number of seeded cells.

BrdU incorporation during DNA synthesis was determined using the 5-Bromo-2′-deoxy-uridine Labeling and Detection Kit I (Roche, Indianapolis, IN, USA). Briefly, cells were seeded at $3.0\times10^4$ cells per well in 48-well culture plates and incubated in D-MEM containing 10% FCS at 37°C for 24 h. After cells were

**Table 1.** PCR primers.

| | Sense | Antisense | Ta | cycles |
|---|---|---|---|---|
| GFAP | 5′-ATCCGCTCAGGTCATCTTACCC-3′ | 5′-TGTCTGCTCAATGTCTTCCCTACC-3′ | 63 | 25 |
| S100β | 5′-AGAGGACTCCAGCAGCAAAGG-3′ | 5′-AGAGAGCTCAGCTCCTTCGAG-3′ | 59 | 32 |
| EAAT1 | 5′-GAAGTCTCCCAGACGTTCTAATCC-3′ | 5′-GCTCTGAAACCGCCACTTACTATC-3′ | 65 | 35 |
| EAAT2 | 5′-ATGCTCATCCTCCCTCTTATCATC-3′ | 5′-CTTTCTTTGTCACTGTCTGAATCTG-3′ | 63 | 32 |
| GS | 5′-TGTACCTCCATCCTGTTGCC-3′ | 5′-GTCCCCGTAATCTTGACTCC-3′ | 57 | 25 |
| HPRT | 5′-CCTGCTGGATTACATTAAAGCACTG-3′ | 5′-AAGGGCATATCCAACAACAA-3′ | 57 | 30 |
| MeCP2 | 5′-GGTAAAACCCGTCCGGAAAATG-3′ | 5′-TTCAGTGGCTTGTCTCTGAG-3′ | 61 | 35 |

GFAP, glial fibrillary acidic protein; EAAT, excitatory amino acid transporter; GS, glutamine synthetase; HPRT, hypoxantine-phosphoribosyl-transferase; MeCP2, methyl-CpG-binding protein 2; Ta, annealing temperature (°C).

doi:10.1371/journal.pone.0035354.t001

incubated with 10 μM BrdU for 2 h, they were fixed with 70% ethanol in 50 mM glycine (pH 2.0) for 20 min at −20°C. Cells were incubated with an anti-BrdU monoclonal antibody, followed by a fluorescein-coupled goat anti-mouse Ig and Hoechst33324 (1 μg/ml). To determine the percentages of BrdU-positive cells, fluorescent images were obtained by a Biorevo BZ-9000 fluorescence microscope (KEYENCE Co., Osaka, Japan); images were analyzed using the BZ-II application. BrdU-positive cells and total cells were counted in random 3 fields per well (approximately 1200 cells per well). Results were obtained from four independent experiments.

## Cell Viability Analysis

Cell were seeded at $1\times10^4$ cells per well in 96-well plates and incubated in D-MEM containing 15% FCS at 37°C for 24 h. In injury models of drug and oxidative stress, cells were incubated with 0.01–10 mM glutamate for 24 h, 12.5–200 mM $NH_4Cl$ (Sigma Chemical Co.) for 4 h, or 0.125–1.0 mM $H_2O_2$ (Wako Pure Chemical Industry, Osaka, Japan) for 1 h as previously described [28,39,40]. After 24 h of drug treatment, cell viability was determined using the WST-8 assay (NACALAI TESQUE, INC., Kyoto, Japan) [39,41].

## PCR analysis

MeCP2$^{-/+}$ female mice (B6.129P2(C)-Mecp2$^{tm1.1Bird}$/J strain) were purchased from the Jackson Laboratory (Bar Harbor, ME) and mated with wild-type C57BL/6 male mice. DNA samples were extracted from tail snips from newborn animals; prior to nucleic acid extraction, snips were digested with proteinase K. Genotyping was performed by PCR analysis of genomic DNA according to the protocol provided by the manufacturer (http://jaxmice.jax.org/pub-cgi/protocols/protocols.sh?objtype=protocol&protocol_id=598) [4,12]. All experiments were performed in accordance with the National Institutes of Health Guidelines for the Care and Use of Laboratory Animals, and were approved by the Animal Research Committee of Kurume University.

Total RNA was extracted from cells using a Sepazol RNA I super kit (Nacalai Tesque, Inc., Kyoto, Japan) [41,42]. One microgram of total RNA was reverse transcribed, and 1/100 of the cDNA (equivalent to 10 ng of total RNA) was subjected to PCR amplification with Taq DNA polymerase (Promega, Co., Ltd., Madison, WI) using the following conditions: 25–35 cycles of 94°C for 30 s, annealing temperature for 60 s, and 74°C for 60 s. Primer sets and annealing temperatures are shown in Table 1. The most appropriate PCR conditions for semi-quantitative analysis of each gene were carefully determined by several preliminary experiments (Fig. S4). The number of cycles for GFAP, S100β, EAAT1, EAAT2, and GS was 25, 32, 35, 32, and 25, respectively (Table 1). The amplified cDNA was electrophoresed on 2% agarose gels containing ethidium bromide, and quantities were analyzed by densitometry using ImageJ software (the Research Service Branch of the National Institute of Health, Bethesda, MD, USA) [42]. The relative expression of each gene was normalized to the intensity of a housekeeping gene, hypoxantine-phosphoribosyl-transferase (HPRT; 30 cycles). The expression level of each gene is reported as a ratio relative to the level of normalized expression in a control sample.

## Immunocytochemistry

Cultures were fixed with 4% paraformaldehyde for 10 min and permeabilized with 0.05% Triton-X 100 for 5 min. After blocking of nonspecific binding sites with 10% nonfat dry milk in PBS for 1 h, cultures were immunocytochemically stained using antibodies against MeCP2 (anti-MeCP2 polyclonal antibody, MILLIPORE, Temecula, CA, USA; anti-MeCP2 monoclonal antibody, G-6, Santa Cruz Biotechnology, Inc., Santa Cruz, CA), β-tubulin type III (TuJ, Sigma-Aldrich, Inc., St. Louis, Missouri), or glial fibrillary acidic protein (GFAP) (anti-GFAP polyclonal antibody, G9269; anti-GFAP monoclonal antibody, G3893, Sigma-Aldrich, Inc., St. Louis, Missouri), followed by secondary fluorescent antibodies as described previously [12]. Cultures were additionally stained with Hoechst33342 and examined using an Olympus IX-70 (Olympus Japan Inc. Tokyo, Japan) microscope. Photomicrographs were captured using an Olympus DP70 digital camera.

## Immunoblotting

Cell extracts were prepared from astroglial cultures as described previously [41]. Western blot analysis was performed using anti-glutamine synthetase (G2781; Sigma-Aldrich, Inc., St. Louis, Missouri), anti-excitatory amino acid transporter 1 (EAAT1, GLAST; Santa Cruz Biotechnology, Inc., Santa Cruz, CA), horseradish peroxidase-conjugated anti-rabbit IgG (DakoCytomation, Glostrup, Denmark), and chemiluminescent substrate (Chemi-Lumi One, NACALAI TESQUE, INC., Kyoto, Japan) [12,41]. Several different exposure times were used for each blot to ensure linearity of band intensities. Immunoreactive bands were quantified using the ImageJ software (Research Service Branch of the National Institute of Health, Bethesda, MD, USA). The relative expression of each protein was normalized to the intensity of β-actin. The expression level of each protein is reported as a

ratio relative to the level of normalized expression in a control sample.

### Glutamate Clearance Assay

To measure extracellular glutamate (Glu) concentrations, we used the Glutamate Assay Kit colorimetric assay (Yamasa Corporation, Tokyo, Japan) [43]. Assays were carried out in six independent trials. The clearance ratio of Glu was calculated from the Glu concentration (μM) in the medium sample of the drug-treated astroglial cells ($Glu_{drug}$) and the control non-drug treated (i.e., treated with drug vehicle alone) glial cells ($Glu_{solv}$). This is represented mathematically as follows: Glu clearance ratio = $(100-Glu_{drug})/(100-Glu_{solv})$. Threo-beta-benzyloxyaspartate (TBOA), UCPH-101 (2-amino-4-(4-methoxyphenyl)-7-(naphthalen-1-yl)-5-oxo-5,6,7,8-tetrahydro-4H-chromene-3-carbonitrile), or dihydrokainate (DHKA) (all purchased from Tocris Bioscience Ellisville, MO, USA) were applied to astroglial cells 60 min before Glu.

### Statistical analysis

Quantitative results are expressed as means ± standard errors (SE). Student's t-test was used to compare data, with $p<0.05$ considered significant.

## Supporting Information

**Figure S1 BrdU-incorporating cells in wild-type and MeCP2-null astrocytes.** The top and bottom pictures show BrdU-incorporating (Green) and Hoechst-stained (Blue) cells, respectively, which were stained with the primary anti-BrdU antibodies, the secondary fluorescein-coupled antibodies, and Hoechst 33324. Negative controls received identical treatments, but were not exposed to BrdU. Representative pictures were used to accurately count the number of BrdU incorporated cells to assess the efficiency of astrocyte cell growth. Scale bar = 200 μm.
(EPS)

**Figure S2 Concentration dependency of GS and EAAT1 expression in wild-type and MeCP2-null astrocytes treated with Glutamate.** The astrocytes of each group were treated with 0.01–1.0 mM Glu for 12 h, and subsequently analyzed for expression of GS and EAAT1 by western blot analysis.
(EPS)

**Figure S3 Purity of astroglial cultures from mouse brain.** The purity of astroglial cultures was assessed by immunocytochemisty (**A**) and immunoblotting (**B**) using antibodies against glial fibrillary acidic protein (GFAP; astrocyte marker; Sigma-Aldrich), CD11b (microglial marker; Santacruz), or microtubule associated protein 2 (MAP2; neuronal marker; Sigma-Aldrich). **A.** Immunocytochemistry indicates that neither CD11b nor MAP2 were expressed in astrocyte cultures. Positive control indicates microglia and mouse ES-derived neural cells that stained with anti-CD11b and MAP2 antibodies, respectively. Scale bar = 100 μm. **B.** Western blot analysis of protein extracts from cultured astrocytes and mouse whole brain. Western blot analysis also confirmed that the cultured astrocytes expressed GFAP, but did not express CD11b and MAP2.
(EPS)

**Figure S4 Optimization of the semi-quantitative RT-PCR assay.** Total RNA extracted from neonatal mouse brain astrocytes was serially diluted (2.5, 5, 10, 20, and 40 ng RNA in lanes 1, 2, 3, 4, and 5, respectively), reverse-transcribed and used as control samples in semi-quantitative RT-PCR for GFAP (**A**), S100β (**B**), HPRT (**C**), EAAT1 (**D**), EAAT2 (**E**), and GS (**F**). PCR was carried out for indicated cycles using each of primer sets shown in Table 1. The amplified cDNA was electrophoresed in a 2% agarose gel containing ethidium bromide. NT, RT-PCR with no template.
(EPS)

**Information S1 Supporting materials and methods.**
(DOC)

## Author Contributions

Conceived and designed the experiments: YO TT. Performed the experiments: YO CM TT. Analyzed the data: YO TT ET. Contributed reagents/materials/analysis tools: KK TM. Wrote the paper: YO TT.

## References


1. Chahrour M, Zoghbi HY (2007) The story of Rett syndrome: from clinic to neurobiology. Neuron 56: 422–437.
2. Matsuishi T, Yamashita Y, Takahashi T, Nagamitsu S (2011) Rett syndrome: The state of clinical and basic research, and future perspectives. Brain Dev 33: 623–631.
3. Amir RE, Van den Veyver IB, Wan M, Tran CQ, Francke U, et al. (1999) Rett syndrome is caused by mutations in X-linked MECP2, encoding methyl-CpG-binding protein 2. Nat Genet 23: 185–188.
4. Guy J, Hendrich B, Holmes M, Martin JE, Bird A (2001) A mouse Mecp2-null mutation causes neurological symptoms that mimic Rett syndrome. Nat Genet 27: 322–326.
5. Chen RZ, Akbarian S, Tudor M, Jaenisch R (2001) Deficiency of methyl-CpG binding protein-2 in CNS neurons results in a Rett-like phenotype in mice. Nat Genet 27: 327–331.
6. Calfa G, Percy AK, Pozzo-Miller L (2011) Experimental models of Rett syndrome based on Mecp2 dysfunction. Exp Biol Med (Maywood) 236: 3–19.
7. Bienvenu T, Chelly J (2006) Molecular genetics of Rett syndrome: when DNA methylation goes unrecognized. Nat Rev Genet 7: 415–426.
8. Saywell V, Viola A, Confort-Gouny S, Le Fur Y, Villard L, et al. (2006) Brain magnetic resonance study of Mecp2 deletion effects on anatomy and metabolism. Biochem Biophys Res Commun 340: 776–783.
9. Ballas N, Lioy DT, Grunseich C, Mandel G (2009) Non-cell autonomous influence of MeCP2-deficient glia on neuronal dendritic morphology. Nat Neurosci 12: 311–317.
10. Maezawa I, Swanberg S, Harvey D, LaSalle JM, Jin LW (2009) Rett syndrome astrocytes are abnormal and spread MeCP2 deficiency through gap junctions. J Neurosci 29: 5051–5061.
11. Maezawa I, Jin LW (2010) Rett syndrome microglia damage dendrites and synapses by the elevated release of glutamate. J Neurosci 30: 5346–5356.
12. Okabe Y, Kusaga A, Takahashi T, Mitsumasu C, Murai Y, et al. (2010) Neural development of methyl-CpG-binding protein 2 null embryonic stem cells: a system for studying Rett syndrome. Brain Res 1360: 17–27.
13. Lioy DT, Garg SK, Monaghan CE, Raber J, Foust KD, et al. (2011) A role for glia in the progression of Rett's syndrome. Nature 475: 497–500.
14. Seifert G, Schilling K, Steinhauser C (2006) Astrocyte dysfunction in neurological disorders: a molecular perspective. Nat Rev Neurosci 7: 194–206.
15. Eroglu C, Barres BA (2010) Regulation of synaptic connectivity by glia. Nature 468: 223–231.
16. Sheldon AL, Robinson MB (2007) The role of glutamate transporters in neurodegenerative diseases and potential opportunities for intervention. Neurochem Int 51: 333–355.
17. Eid T, Williamson A, Lee TS, Petroff OA, de Lanerolle NC (2008) Glutamate and astrocytes–key players in human mesial temporal lobe epilepsy? Epilepsia 49 Suppl 2: 42–52.
18. Hamberger A, Gillberg C, Palm A, Hagberg B (1992) Elevated CSF glutamate in Rett syndrome. Neuropediatrics 23: 212–213.
19. Lappalainen R, Riikonen RS (1996) High levels of cerebrospinal fluid glutamate in Rett syndrome. Pediatr Neurol 15: 213–216.
20. Pan JW, Lane JB, Hetherington H, Percy AK (1999) Rett syndrome: 1H spectroscopic imaging at 4.1 Tesla. J Child Neurol 14: 524–528.
21. Horska A, Farage L, Bibat G, Nagae LM, Kaufmann WE, et al. (2009) Brain metabolism in Rett syndrome: age, clinical, and genotype correlations. Ann Neurol 65: 90–97.
22. Ward BC, Kolodny NH, Nag N, Berger-Sweeney JE (2009) Neurochemical changes in a mouse model of Rett syndrome: changes over time and in response to perinatal choline nutritional supplementation. J Neurochem 108: 361–371.

23. Viola A, Saywell V, Villard L, Cozzone PJ, Lutz NW (2007) Metabolic fingerprints of altered brain growth, osmoregulation and neurotransmission in a Rett syndrome model. PLoS One 2: e157.
24. Dunn HG, MacLeod PM (2001) Rett syndrome: review of biological abnormalities. Can J Neurol Sci 28: 16–29.
25. Naidu S, Kaufmann WE, Abrams MT, Pearlson GD, Lanham DC, et al. (2001) Neuroimaging studies in Rett syndrome. Brain Dev 23 Suppl 1: S62–71.
26. Colantuoni C, Jeon OH, Hyder K, Chenchik A, Khimani AH, et al. (2001) Gene expression profiling in postmortem Rett Syndrome brain: differential gene expression and patient classification. Neurobiol Dis 8: 847–865.
27. Setoguchi H, Namihira M, Kohyama J, Asano H, Sanosaka T, et al. (2006) Methyl-CpG binding proteins are involved in restricting differentiation plasticity in neurons. J Neurosci Res 84: 969–979.
28. Chen CJ, Liao SL, Kuo JS (2000) Gliotoxic action of glutamate on cultured astrocytes. J Neurochem 75: 1557–1565.
29. Lehmann C, Bette S, Engele J (2009) High extracellular glutamate modulates expression of glutamate transporters and glutamine synthetase in cultured astrocytes. Brain Res 1297: 1–8.
30. Shigeri Y, Seal RP, Shimamoto K (2004) Molecular pharmacology of glutamate transporters, EAATs and VGLUTs. Brain Res Brain Res Rev 45: 250–265.
31. Erichsen MN, Huynh TH, Abrahamsen B, Bastlund JF, Bundgaard C, et al. (2010) Structure-activity relationship study of first selective inhibitor of excitatory amino acid transporter subtype 1: 2-Amino-4-(4-methoxyphenyl)-7-(naphthalen-1-yl)-5-oxo-5,6,7,8-tetrahydro-4 H-chromene-3-carbonitrile (UCPH-101). J Med Chem 53: 7180–7191.
32. Deguchi K, Antalffy BA, Twohill LJ, Chakraborty S, Glaze DG, et al. (2000) Substance P immunoreactivity in Rett syndrome. Pediatr Neurol 22: 259–266.
33. Namihira M, Nakashima K, Taga T (2004) Developmental stage dependent regulation of DNA methylation and chromatin modification in a immature astrocyte specific gene promoter. FEBS Lett 572: 184–188.
34. Tsujimura K, Abematsu M, Kohyama J, Namihira M, Nakashima K (2009) Neuronal differentiation of neural precursor cells is promoted by the methyl-CpG-binding protein MeCP2. Exp Neurol 219: 104–111.
35. Jellinger K, Armstrong D, Zoghbi HY, Percy AK (1988) Neuropathology of Rett syndrome. Acta Neuropathol 76: 142–158.
36. Kim SY, Choi SY, Chao W, Volsky DJ (2003) Transcriptional regulation of human excitatory amino acid transporter 1 (EAAT1): cloning of the EAAT1 promoter and characterization of its basal and inducible activity in human astrocytes. J Neurochem 87: 1485–1498.
37. Yang Y, Gozen O, Vidensky S, Robinson MB, Rothstein JD (2010) Epigenetic regulation of neuron-dependent induction of astroglial synaptic protein GLT1. Glia 58: 277–286.
38. Ricciardi S, Boggio EM, Grosso S, Lonetti G, Forlani G, et al. (2011) Reduced AKT/mTOR signaling and protein synthesis dysregulation in a Rett syndrome animal model. Hum Mol Genet 20: 1182–1196.
39. Ushikoshi H, Takahashi T, Chen X, Khai NC, Esaki M, et al. (2005) Local overexpression of HB-EGF exacerbates remodeling following myocardial infarction by activating noncardiomyocytes. Lab Invest 85: 862–873.
40. Norenberg MD, Jayakumar AR, Rama Rao KV, Panickar KS (2007) New concepts in the mechanism of ammonia-induced astrocyte swelling. Metab Brain Dis 22: 219–234.
41. Takahashi T, Kawai T, Ushikoshi H, Nagano S, Oshika H, et al. (2006) Identification and isolation of embryonic stem cell-derived target cells by adenoviral conditional targeting. Mol Ther 14: 673–683.
42. Kawai T, Takahashi T, Esaki M, Ushikoshi H, Nagano S, et al. (2004) Efficient cardiomyogenic differentiation of embryonic stem cell by fibroblast growth factor 2 and bone morphogenetic protein 2. Circ J 68: 691–702.
43. Takeuchi H, Mizuno T, Zhang G, Wang J, Kawanokuchi J, et al. (2005) Neuritic beading induced by activated microglia is an early feature of neuronal dysfunction toward neuronal death by inhibition of mitochondrial respiration and axonal transport. J Biol Chem 280: 10444–10454.

CLINICAL GENETICS
An International Journal of Genetics, Molecular and Personalized Medicine

*Clin Genet 2012: 82: 569–573*
*Printed in Singapore. All rights reserved*



CLINICAL GENETICS
doi: 10.1111/j.1399-0004.2011.01819.x

## Short Report

# *FOXG1* mutations in Japanese patients with the congenital variant of Rett syndrome

**S Takahashi[a], N Matsumoto[a], A Okayama[a], N Suzuki[a], A Araki[a], K Okajima[a], H Tanaka[b] and A Miyamoto[b]**

[a]Department of Pediatrics, Asahikawa Medical University, Asahikawa, Japan and [b]Department of Pediatrics, Asahikawa Habilitation Center for Disabled Children, Asahikawa, Japan

Takahashi S, Matsumoto N, Okayama A, Suzuki N, Araki A, Okajima K, Tanaka H, Miyamoto A. *FOXG1* mutations in Japanese patients with the congenital variant of Rett syndrome.
Clin Genet 2012: 82: 569–573. © John Wiley & Sons A/S. Published by Blackwell Publishing Ltd, 2011

Rett syndrome (RTT) is a severe neurodevelopmental disorder characterized by microcephaly, psychomotor regression, seizures and stereotypical hand movements. Recently, deletions and inactivating mutations in *FOXG1*, encoding a brain-specific transcription factor that is critical for forebrain development, have been found to be associated with the congenital variant of RTT. Here we report the clinical features and molecular characteristics of two cases of the congenital variant of RTT. We conducted mutation screenings of *FOXG1* in a cohort of 15 Japanese patients with a clinical diagnosis of atypical RTT but without *MECP2* and *CDKL5* mutations. Two unrelated female patients had heterozygous mutations (c.256dupC, p.Gln86ProfsX35 and c.689G>A, pArg230His). Both showed neurological symptoms from the neonatal period, including hypotonia, irritability and severe microcephaly. Further, their psychomotor development was severely impaired, as indicated by their inability to sit unaided or acquire speech sounds, and they had a hyperkinetic movement disorder, because both displayed hand stereotypies and jerky movements of the upper limbs. Brain magnetic resonance imaging scans revealed delayed myelination with hypoplasia of the corpus callosum and frontal lobe. These cases confirm the involvement of FOXG1 in the molecular etiology of the congenital variant of RTT and show the characteristic features of FOXG1-related disorder.

**Conflict of interest**

The authors declare no conflicts of interest.

Key words: congenital variant – *FOXG1* – microcephaly – mutation – Rett syndrome

Corresponding author: Satoru Takahashi, MD, PhD, Department of Pediatrics, Asahikawa Medical University, 2-1-1-1 Midorigaoka-Higashi, Asahikawa, Hokkaido 078–8510, Japan.
Tel.: +81 166 68 2483;
fax: +81 166 68 2489;
e-mail: satoru5p@asahikawa-med.ac.jp

Received 6 September 2011, revised and accepted for publication 28 November 2011

Rett syndrome (RTT) is a neurodevelopmental disorder that is associated with mutations in *MECP2*, encoding methyl-CpG-binding protein 2 (1). Patients with RTT show characteristic clinical features including hypotonia, developmental delay, loss of purposeful hand movements, hand stereotypies and decelerated head growth (2). The clinical severity of RTT varies widely, ranging from the severe 'congenital variant' to the milder 'forme fruste' (3). The congenital variant is characterized by hypotonia and developmental delay beginning earlier than in the typical RTT. *MECP2* mutations are present in 70–90% of the typical RTT cases, but the mutation rate is low in atypical RTT cases (4), suggesting that other genes are responsible for the atypical forms.

Small *de novo* interstitial deletions in 14q12 and a balanced *de novo* translocation [t(2;14)(p22;q12)] with an adjacent small inversion in 14q12 have been identified in cases with clinical features reminiscent of the congenital variant of RTT (5–8). The common deleted region contains *FOXG1*, a gene that encodes a brain-specific transcriptional repressor FOXG1, which promotes progenitor proliferation and suppresses premature neurogenesis for proper forebrain development (9, 10). Both *FOXG1* homozygous- and heterozygous-mutant mice exhibit complex forebrain malformations (9–12). The importance of *FOXG1* was reinforced by the identification of *FOXG1*-null mutations in two unrelated girls with the congenital variant (13). These studies suggest that the congenital

variant of RTT can be caused by point mutations as well as complete deletions in *FOXG1*.

At present, 17 point mutations in *FOXG1* have been reported in patients with the congenital variant of RTT (13–20). Here, we report two *FOXG1* mutations associated with the congenital variant, which confirms the involvement of FOXG1 in the pathophysiology of the congenital variant of RTT and helps to delineate the clinical features associated with *FOXG1* mutations.

## Materials and methods

### Patients

Fifteen Japanese patients (13 females and 2 males) with a clinical diagnosis of atypical RTT based on the revised criteria for this disorder (2) were examined. Eight and seven patients were considered to have the congenital and early seizure variants, respectively. Direct sequencing of the entire coding sequences and exon–intron boundaries did not reveal *MECP2* and *CDKL5* mutations in these patients. The possibility of large rearrangements in these genes was excluded by using multiplex ligation-dependent probe amplification (MLPA) method (MRC-Holland, Amsterdam, The Netherlands).

### Molecular analysis

Blood samples were collected from the patients and their parents after their written informed consent. Genomic DNA was extracted from peripheral blood leukocytes and used as the template for polymerase chain reaction (PCR). Appropriate primers were used to yield DNA fragments spanning the entire *FOXG1* coding region (13). Mutation screenings were performed by direct sequencing of exon1-derived PCR products. Large rearrangements of *FOXG1* DNA were detected by using the MLPA method according to the manufacturer's instructions (MRC-Holland).

## Results

### Case report

#### *Patient 1*

This female patient, now aged 34 years, is the third child of healthy and non-consanguineous parents. She has two healthy brothers. She was born at term by spontaneous delivery after an uneventful pregnancy. Her birth weight was 2570 g and she had a small occipito-frontal circumference (OFC) of 30 cm (third percentile). During the neonatal period, she showed sleep disturbance and inconsolable crying. She was referred to a clinical unit at 7 months of age because of psychomotor retardation. Physical examination revealed severe hypotonia, poor eye contact, strabismus and head growth deceleration. At the age of 1 year, she displayed hand stereotypies with hand-to-mouth movements, tongue protrusion and intermittent bruxism. She also had generalized tonic seizures at that age. Interictal electroencephalogram (EEG) showed focal spike discharges over the left parietal area. The seizures were eventually controlled with sodium valproate and clobazam. Because of feeding problems resulting from swallowing difficulties, she was fed predominantly via a gastrostomy tube. She was never able to sit unaided and never acquired speech sounds or purposeful hand skills. At present, she is permanently bedridden and has severe scoliosis, jerky movements of the upper limbs, self-abusive behavior such as biting her hands and microcephaly (OFC of 46 cm). Brain magnetic resonance imaging (MRI) scans performed at the age of 33 years showed microcephaly with hypoplasia of the frontal lobes and corpus callosum (Fig. 1a,b).

#### *Patient 2*

This 8-year-old female patient is the second child of healthy and non-consanguineous parents. She has a healthy brother. She was born at term by spontaneous delivery after an uneventful pregnancy. Her birth weight was 2686 g and she had a relatively small head circumference (OFC of 31 cm; 10th percentile). During the neonatal period, she had strabismus, poor eye contact and inconsolable crying. She was referred to a clinical unit at 2 months of age. Physical examination revealed severe hypotonia and decelerated head growth. Microcephaly became more evident with time (OFCs of 38, 41, 43 and 44 cm at 6 months, 2, 5 and 7 years, respectively, all below the third percentile). The developmental milestones were severely delayed: she acquired head control at 7 months and turned over at 20 months. She displayed prominent hyperkinetic movement disorders with hand stereotypies, jerky movements of the upper limbs and frequent and inappropriate episodes of laughter. At 3 years of age, she had two episodes of hyperthermia-induced seizures. Although interictal EEG revealed focal spike discharges over the right parietal area, the seizures did not recur even without antiepileptic drug treatment. She remains incapable of sitting up unaided, as well as acquiring speech sounds and purposeful hand skills. Brain MRI scans performed at the age of 8 years showed delayed myelination in the frontal lobe with hypoplasia of the corpus callosum and frontal lobe (Fig. 1c,d).

### Identification of *FOXG1* mutations

We identified heterozygous *FOXG1* mutations in both patients (Fig. 2). Patient 1 showed duplication of cytosine at nucleotides 256 (c.256dupC, p.Gln86ProfsX35), resulting in the loss of the three main functional domains of FOXG1 (Fig. 2a). This frameshift mutation has also been identified in an unrelated patient (20). Patient 2 showed a novel missense mutation (c.689G>A, p.Arg230His) within the DNA-binding forkhead domain, which affects a residue highly conserved in different species (Fig. 2b). Testing of their parents confirmed that both the mutations were *de novo*. We did not find deletions in *FOXG1* in our cohort.

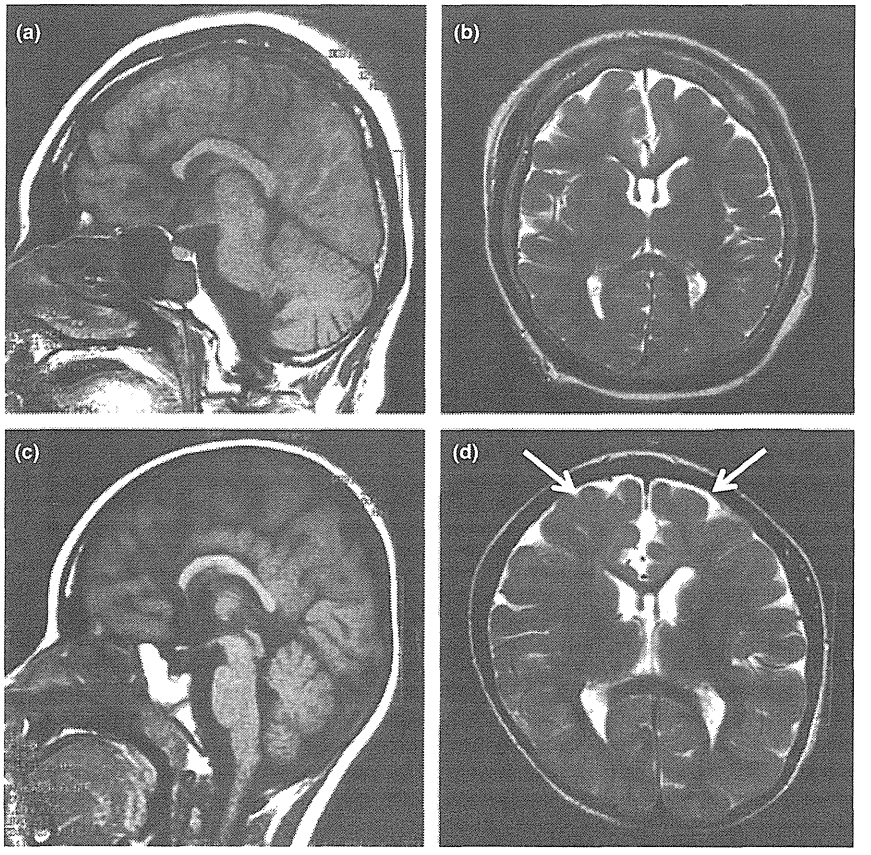


*Fig. 1.* Brain magnetic resonance imaging (MRI) scans of the two patients with *FOXG1* mutations. Patient 1 (aged 33 years during MRI) has hypoplasia of the frontal lobe and corpus callosum (**a** and **b**). Patient 2 (aged 8 years during MRI) has delayed myelination in the frontal lobe (arrows) with hypoplasia of the corpus callosum and frontal lobe (**c** and **d**). Both have a low forehead which indicates a hypoplastic frontal lobe. (**a**) and (**c**) T1-weighted sagittal images; (**b**) and (**d**) T2-weighted axial images.

## Discussion

We identified two heterozygous *FOXG1* mutations in two patients with the congenital variant of RTT. These new cases provide additional support for delineating the clinical features of the FOXG1-related phenotypes. Both the patients had hypotonia and irritability in the neonatal period. Deceleration of head growth, leading to severe microcephaly, was recognized soon afterwards. They also had strabismus and poor eye contact. Their motor development was severely impaired and voluntary hand use was absent. They were unable to sit unaided and did not acquire speech sounds. They showed a prominent hyperkinetic movement disorder, with hand stereotypies and jerky movements of the upper limbs. These clinical features are similar to those previously described in patients with the congenital variant of RTT (13–20).

Large-scale molecular screenings of *FOXG1* have been conducted mainly in female individuals with typical and atypical RTT (14–16). The preponderance of female patients with *FOXG1* mutations may be because of this bias. Recent studies have shown point mutations and deletions in 14q12 in male individuals with the congenital variant of RTT as well (17, 20). Given that *FOXG1* is an autosomal gene, *FOXG1* mutations may be responsible for the clinical features in female and male individuals with this form of RTT. The c.256dupC mutation has been identified in a male patient who presented similar clinical features to those observed in our female patient (20). This recurrent mutation caused duplication of cytosine after seven subsequent cytosines in *FOXG1*, suggesting that this cytosine stretch may be prone to replication errors and present a mutation hotspot in *FOXG1*.

FOXG1 is a DNA-binding transcription factor with a forkhead domain that represses target genes. It recruits transcriptional co-repressor proteins via two protein-binding domains (JARID1B and Groucho-binding domains). Interaction between FOXG1 and its co-repressor proteins is critical for early brain development (21). Missense mutations in the functional domains of FOXG1 or late truncating mutations possibly cause a milder phenotype, because the resulting proteins may retain some functions (16). However, Patient 2, who had a missense mutation of the DNA-binding forkhead domain, presented with a severe phenotype similar to that of Patient 1, who harbored a frameshift mutation that resulted in the loss of the three main

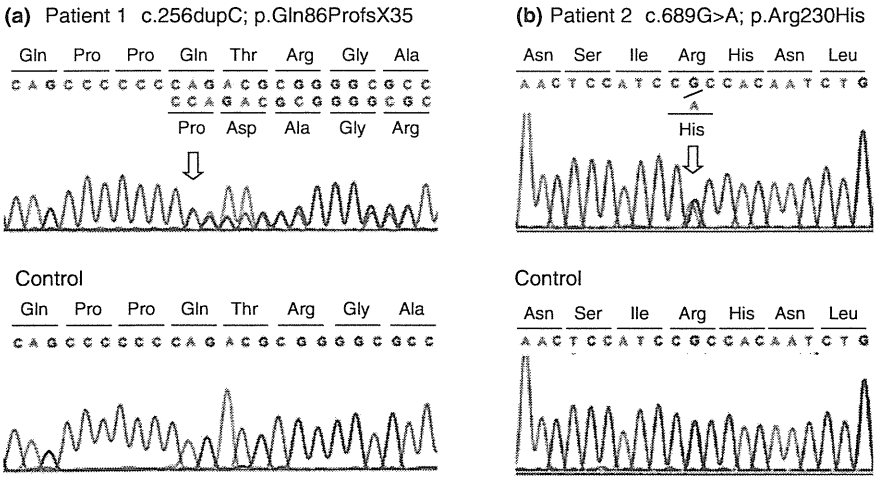


*Fig. 2.* The *FOXG1* mutations in Patients 1 and 2. Automated DNA sequencing with the polymerase chain reaction product from Patient 1 showed duplication of cytosine at nucleotides 256 (c.256dupC, numbering according to GenBank accession no. NM_005249.3) in *FOXG1* (arrow), which resulted in a shift of the reading frame and introduction of a premature stop codon (p.Gln86ProfsX35) (**a**). In Patient 2, we found a guanine-to-adenine transition at nucleotide 689 (c.689G>A), which resulted in an arginine-to-histidine substitution at amino acid position 230 (p.Arg230His; arrow) (**b**).

functional domains of FOXG1. The missense mutation (p.Arg230His) appeared to affect the affinity of FOXG1 for DNA. Our findings support the idea that a missense mutation in the forkhead domain impairs its target recognition and causes mislocalization of the protein in the nucleus (19). Thus, missense mutations within the DNA-binding domain, as well as clear loss-of-function mutations, can have a severe impact on FOXG1 function. Our data, taken together with previous findings, indicate that the genotype does not predict the severity of the phenotype. Indeed, a late truncating mutation (p.Tyr416X) that affects the C-terminal part of FOXG1 but maintains the three known functional domains reportedly causes the most severe phenotype (14).

FOXG1 plays an important role in forebrain development (10). Brain MRI scans of our two patients showed poor development of the frontal lobe and hypoplasia of the corpus callosum, which are similar to the findings of previous *FOXG1* mutation reports (14, 15, 20). *FOXG1* mutant mice are an interesting animal model for investigating how *FOXG1* haploinsufficiency affects brain development and neuronal function. Although *FOXG1* homozygous-mutant mice die shortly after birth with severe brain defects (9), the heterozygous mutants have less severe brain defects but still exhibit a reduction in the volume of the neocortex, hippocampus and striatum and a thin cortex because of reduced thickness of the superficial cortical layers (12). Furthermore, *FOXG1* heterozygous-mutant mice exhibit learning deficits in fear-condition behavioral tests (11). These animal data are consistent with the findings that humans with *FOXG1* haploinsufficiency have poor forebrain development as well as cognitive and motor defects.

In conclusion, we identified a novel mutation and a recurrent mutation in *FOXG1* in two patients with the congenital variant of RTT. Our data support the involvement of FOXG1 in the molecular etiology of this form of RTT. We suggest that *FOXG1* mutation analysis should be performed in female and male patients with developmental features suggestive of the congenital variant and brain malformations including poor frontal lobe development and hypoplasia of the corpus callosum.

## Acknowledgements

We thank the families described here, whose help and participation made this work possible. This work was supported in part by Grant-in-Aid for Scientific Research C from the Japan Society for the Promotion of Science (#22591118).

## References

1. Amir RE, Van den Veyver IB, Wan M, Tran CQ, Francke U, Zoghbi HY. Rett syndrome is caused by mutations in X-linked MECP2, encoding methyl-CpG-binding protein 2. Nat Genet 1999: 23: 185–188.
2. Neul JL, Kaufmann WE, Glaze DG et al. Rett syndrome: revised diagnostic criteria and nomenclature. Ann Neurol 2010: 68: 944–950.
3. Hagberg BA, Skjeldal OH. Rett variants: a suggested model for inclusion criteria. Pediatr Neurol 1994: 11: 5–11.
4. Webb T, Latif F. Rett syndrome and the MECP2 gene. J Med Genet 2001: 38: 217–223.
5. Shoichet SA, Kunde SA, Viertel P et al. Haploinsufficiency of novel FOXG1B variants in a patient with severe mental retardation, brain malformations and microcephaly. Hum Genet 2005: 117: 536–544.
6. Bisgaard AM, Kirchhoff M, Tumer Z et al. Additional chromosomal abnormalities in patients with a previously detected abnormal karyotype, mental retardation, and dysmorphic features. Am J Med Genet A 2006: 140: 2180–2187.
7. Jacob FD, Ramaswamy V, Andersen J, Bolduc FV. Atypical Rett syndrome with selective FOXG1 deletion detected by comparative genomic hybridization: case report and review of literature. Eur J Hum Genet 2009: 17: 1577–1581.
8. Mencarelli MA, Kleefstra T, Katzaki E et al. 14q12 Microdeletion syndrome and congenital variant of Rett syndrome. Eur J Med Genet 2009: 52: 148–152.

9. Xuan S, Baptista CA, Balas G, Tao W, Soares VC, Lai E. Winged helix transcription factor BF-1 is essential for the development of the cerebral hemispheres. Neuron 1995: 14: 1141–1152.
10. Hanashima C, Li SC, Shen L, Lai E, Fishell G. Foxg1 suppresses early cortical cell fate. Science 2004: 303: 56–59.
11. Shen Q, Wang Y, Dimos JT et al. The timing of cortical neurogenesis is encoded within lineages of individual progenitor cells. Nat Neurosci 2006: 9: 743–751.
12. Eagleson KL, Schlueter Mc, Fadyen-Ketchum LJ, Ahrens ET et al. Disruption of Foxg1 expression by knock-in of cre recombinase: effects on the development of the mouse telencephalon. Neuroscience 2007: 148: 385–399.
13. Ariani F, Hayek G, Rondinella D et al. FOXG1 is responsible for the congenital variant of Rett syndrome. Am J Hum Genet 2008: 83: 89–93.
14. Bahi-Buisson N, Nectoux J, Girard B et al. Revisiting the phenotype associated with FOXG1 mutations: two novel cases of congenital Rett variant. Neurogenetics 2010: 11: 241–249.
15. Mencarelli MA, Spanhol-Rosseto A, Artuso R et al. Novel FOXG1 mutations associated with the congenital variant of Rett syndrome. J Med Genet. 2010: 47: 49–53.
16. Philippe C, Amsallem D, Francannet C et al. Phenotypic variability in Rett syndrome associated with FOXG1 mutations in females. J Med Genet 2010: 47: 59–65.
17. Kortüm F, Das S, Flindt M et al. The core FOXG1 syndrome phenotype consists of postnatal microcephaly, severe mental retardation, absent language, dyskinesia, and corpus callosum hypogenesis. J Med Genet 2011: 48: 396–406.
18. Roche-Martinez A, Gerotina E, Armstrong-Moron J, Sans-Capdevila O, Pineda M. FOXG1, a new gene responsible for the congenital form of Rett syndrome. Rev Neurol 2011: 52: 597–602.
19. Le Guen T, Fichou Y, Nectoux J et al. A missense mutation within the fork-head domain of the forkhead box G1 gene (FOXG1) affects its nuclear localization. Hum Mutat 2011: 32: E2026–E2035.
20. Le Guen T, Bahi-Buisson N, Nectoux J et al. A FOXG1 mutation in a boy with congenital variant of Rett syndrome. Neurogenetics 2011: 12: 1–8.
21. Yao J, Lai E, Stifani S. The winged-helix protein brain factor 1 interacts with groucho and hes proteins to repress transcription. Mol Cell Biol 2001: 21: 1962–1972.